AALBORG UNIVERSITY

The School of Engineering and Science
Sohngårdsholmsvej 57
9000 Aalborg
Telephone: 9940 8530
http://ses.aau.dk

Title: Stochastic Modelling of Soil

Project period: Fall semester 2011

Project group: B122

Jens Saugmann Rasmussen

Rasmus Neigaard Lund Jensen

Synopsis:

The project group will through this report investigate the uncertainties regarding fatigue design of a wind turbine jolt. The test series forming the background of [Eurocode 1993-1-9, 2005] are analysed, and the significance of the scatter included is evaluated. A nonlinear SN-curve is implemented due to the uncertainties regarding the location of the knee point of bilinear SN-curves. Estimates of a Low Cycle Fatigue load is proposed, and the resulting accumulated reliability is analysed by a probabilistic approach. This is done in order to quantify the possible trimming of design parameters, when designing for Fatigue loads.

Number of copies: 5

Number of pages: 39

Deadline: 6. Januar 2012 [1]

Preface

This report is the master thesis by group B121b, as part of the Master programme in Structural and Civil Engineering, 4th semester under the School of Engineering and Science at Aalborg University. The project spans from 2nd of February 2012 until 8th of June 2012. The theme of the thesis is *Stochastic modelling of uncertainties of SN-curves* and the project is executed in accordance with the guidelines given in the Study Programme Guide. To answer the problem statement, the project group has independently, with the help from the supervisor, gathered information about the relevant topics. This knowledge will be documented and evaluated in this report, and later be defended at a presentation and an exam.

Figures and Table numbering is based on which chapter, Figure and Table it can be found at. Sources are noted using the Harvard method. Hereby sources regarding literature, magazines, web pages, programs, and figures are noted as eg. [Dyrbye and Hansen, 1997]. If the source is placed before a full stop, it only refers to the last sentence, whereas a source placed after a full stop refers to the whole paragraph. It should be noted that figures and tables without attached source are own productions. In the bibliography further information about the sources can be found.

All Monte Carlo and First Order Reliability Method calculations are made in FORTRAN, based on files programmed by Prof. John Dalsgaard Sørensen, later modified by the authors of this report.

Table of Contents

1 Introduction

With fear for man-made climate changes, the environmental impact of e.g. the BP and Exxon Valdez accidents, and the unwillingness to depend on imported fossil fuels, renewable energy is catching more and more interest worldwide. Of these renewable energy sources, wind power is one of the most promising, with large projects going on in Europe, North- and South America, and Asia. To promote the construction of wind farms, governments have been backing up the projects with additional fundings for several years. This subsidy has been necessary, in order to encourage the development of cost-efficient wind turbines, which can be competitive with the traditional power plants. The price per kWh produced by wind turbines have steadily decreased the last 30 years with the improvements in the design of the blades, the implementation of control systems, and the general increase in size of wind turbines.

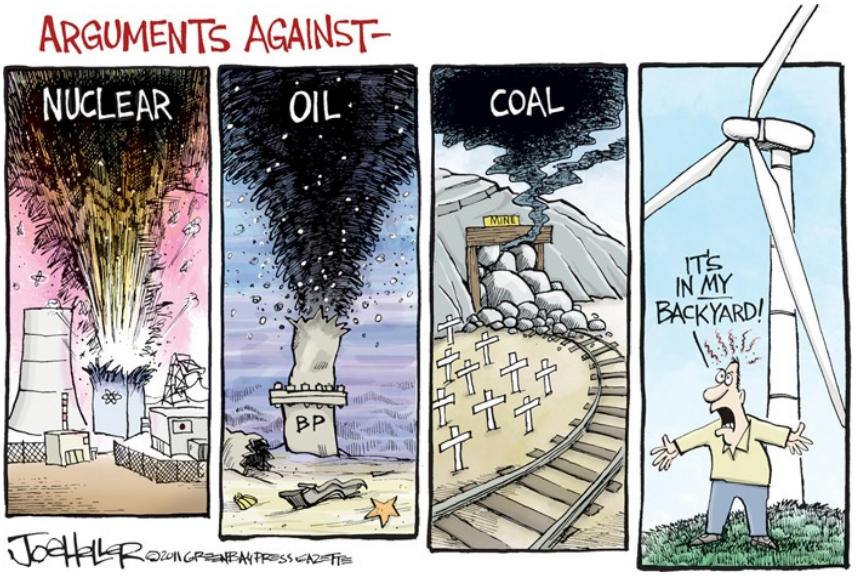

Figure 1.1: Arguments against different types of power productions.

Further reduction in the cost of energy, *COE*, is however still necessary, in order to make the definitive breakthrough for wind energy. The *COE* is defined by Equation (1.1)

$$COE = \frac{Energy}{APEX + OPEX} \tag{1.1}$$

where

$APEX$	Initial expenses of facility
$OPEX$	Operational expenses

To decrease the *COE*, a larger energy output is needed, or a decrease in expenses. The first can be achieved by improving the gearing system, better site assessments, or more efficient aerodynamics of the blades. The latter

can be reached with a trimming of the design, reducing the material consumption, or lower the cost of operation and maintenance of the turbine. Trimming the design can naturally only be done to a certain extent, since a paper thin steel tower supporting a 5 MW wind turbine is likely to fail quite a lot. The key is to reach a design which is precisely strong enough, with a minimum of extra bearing capacity. This being said, a design which is precisely strong enough does not mean that the structure will never fail. If the cost of making the structure stronger is greater than cost of a failure once in a while, this could mean that the chosen design is allowed to fail at a certain probability. This economical criteria assumes of course that the environmental consequences and the risk of loosing human lives in case of failure can be neglected.

1.1 Scope and limitations

The cyclic nature of wind and wave loads on wind turbines means that designing for fatigue is an issue that is highly relevant. Most design codes are using SN-curves with a linear correlation in a log-scale between the magnitude of stress ranges and the number of cycles before failure. The SN-curves are the best available theory to describe the fatigue bearing capacity, but is not very exact. Even with loads perfectly known, results obtained are easily off by a factor 2 or more. One of the reasons why the theory fails to describe reality could be the linear correlation between stress ranges and number of cycles to failure, in a lognormal diagram. The influence of the few very large stress ranges has not yet been analysed thoroughly, even though the topic has been mentioned in some publications. An interesting algorithm is found [Larsen, G. C. and Thomsen, K , 1996], which presents a theoretical approach to describe the effect of Low Cycle Fatigue loads, further on abbreviated to LCF. This theory will be implemented for a connection in a wind turbine, for which load series are found by simulations, using the programs TurbSim [B. J. Jonkman, M. L. Buhl Jr., b] and FAST [B. J. Jonkman, M. L. Buhl Jr., a]. The fatigue damage, including the contribution from the low cycle loads, will be compared with the one obtained from the traditional SN curve based method. Besides LCF, the uncertainties regarding the SN-curves proposed by [Eurocode 1993-1-9, 2005] will be analysed. The test data forming the basis of the code will be presented, and different SN-curves proposed, based on these. Hence the scope of this project is captured in the following:

"'How significant is the impact on the fatigue load for a wind turbine, due to Low Cycle Fatigue, analysed by a probabilistic approach?"'

and

"'How are the uncertainties regarding fatigue life implemented in the SN-curves in [Eurocode 1993-1-9, 2005], and what is the impact on the reliability if other curves are proposed?"'

The resulting reliability of the wind turbine including the contribution from LCF load will be compared to the reliability of a wind turbine designed without. For simplicity, the load case used in this project is not considering wave loads. However, since the theory in [Larsen, G. C. and Thomsen, K , 1996] is based on a load series, it is possible to apply for wave loads, if wanted. With the lack of accuracy of the SN-curves to describe the damage, the test data from which the EC is based is analysed, with the purpose of modelling the SN-curve stochastic.

1.2 Structure of report

The report consist of 10 Chapters, which are divided further into sections and subsections. Chapter 2 contains the theory applied and limitations for determining the wind load. In Chapter 3 the concepts of SN-curves and damage summation is explained, and the test data from which the SN-curves origin is analysed. A probabilistic modelling of the damage calculation is introduced.
Three different methods are proposed in Chapter 4 to determine characteristic SN-curves, and a code based design of a connection is made in Chapter 5. An algorithm from [Larsen, G. C. and Thomsen, K , 1996] is presented in Chapter 6 to implement the contribution from Low cycle fatigue. The theory described in previous Chapters are used to assemble a load series, for which the damage is found.
Instead of the linear SN-curves proposed by [Eurocode 1993-1-9, 2005], a non-linear curve proposed by [Lassen, T. et al , 2005] is presented in Chapter 7. The reliability obtained designing with this curve is compared to the code based.
In Chapter 8 the background tests from which [Eurocode 1993-1-9, 2005] is presented, and an analysis is performed to propose new SN-curves. A sensitivity analysis is made for the stochastic variables modelling the uncertainties in Chapter 9.

Loads

2

In this chapter the wind parameters for obtaining a response from a wind turbine will be presented. Due to the complexity of the wind, simplifications are needed. In this chapter, the wind parameters for obtaining the response for a wind turbine is presented. With the simplifications made, two programs can be used to determine the response of the wind turbine: Turbsim generates windfield series, whereas FAST determines the response of the wind turbine, based on the simulated wind field series.

2.1 Modeling of wind fields

The design lifetime of the wind turbine is set to 20 years in most design situations [Vestas, 2012]. To ensure the safety of the wind turbine the response over the entire life time is therefore needed to count all stress cycles the different components will experience. In an ideal situation the response would be based on measurements over at least 20 years. In reality, this is however seldom possible. Instead, computer simulations are used to propose wind series, from which the response can be found..
But two problems quickly occurs: The amount of data needed for describing the wind field series for 20 year, is extremely data-heavy, and makes it hard to handle calculation-wise. Instead assumptions are made to bring data and time consumption down. One step is to make use of the fact that the metrological conditions repeat them selfs are a period of time. In this report, the wind fields are modelled as series of 10 minutes each. For each 10 minute interval the short term fluctuations are well described by a turbulence model.

$$I(U) = \frac{\sigma_U}{U} = I_{ref}\left(0.75\frac{c_{90\%}}{U}\right) \tag{2.1}$$

where

I	Characteristic turbulence intensity [-]
$c_{90\%}$	Constant = 5.6 [m/s]
I_{ref}	Reference turbulence intensity (offshore = 0.12) [-]
U	Mean wind speed at hub hight [m/s]
σ_U	Turbulence [m/s]

The power in the turbulence is defined by a power spectral density function. A simple and commonly used spectral density with the correct high-frequency behaviour was proposed by Kaimal, [Dyrbye and Hansen, 1997], and is the one used in this report to model the wind fields.
To model the wind fields a commercial software, TurbSim [B. J. Jonkman, M. L. Buhl Jr., b] is used. TurbSim generates series of wind fields, given a mean wind speed and meteorological boundary conditions, (turbulence model, height of reference wind speed, roughness length, etc.).
The wind fields are modelled by mean wind speeds ranking from 3 to 25 m/s with bins of 2m/s. A square with dimensions two times rotor radius + two times shaft length is chosen, to ensure that the wind turbine does not move out of the boundaries of the wind fields. A time step for the sampling frequency is set to 0.05s, as recommended by [B. J. Jonkman, M. L. Buhl Jr., 2008].
These wind field series are then used as input files to FAST, which then gives the response of the wind turbine. Further knowledge about the programs can be gained from [B. J. Jonkman, M. L. Buhl Jr., 2008] and [B. J. Jonkman,

M. L. Buhl Jr., 2005].

The wind turbine chosen to investigate is the one set to standard by FAST. This wind turbine model is composed of data from a number of wind turbine models, since enough details could not be obtained for one specific model. The result is a 'composite' 5 MW wind turbine. Even though some data is used from offshore wind turbines, wave induced loads will not be included. The main characteristics of the turbine can be seen at Table 2.1, as well as some terrain and meteorological conditions.

Parameter	Value
Hub height	90 [m]
Rotor radius	61.5 [m]
Number of blades	3 [-]
Cut in wind speed	3 [m/s]
Cut out wind speed	25 [m/s]
Rated wind speed	11.4 [m/s]
Tower width, top	3.87 [m]
Tower width, bot	6 [m]
Turbulence model	Kaimal

Table 2.1: Characteristics of wind turbine.

By using the inputs above, 72 time series are made to describe the wind fields affecting the turbine. These concist of 6x10 min for each mean wind speed, in the range previously described. With the necessary input data for FAST obtained, the response of the wind turbine can be found. Since the input data is divided in time series for each mean wind speed, so is the output.

2.2 Wind Speed Distrubution

To determine how many of each 10 minutes wind speed series occur in 20 years a weibull distribution is used, see Equation (2.2).

$$P(V_{hub}) = 1 - \exp\left(-\pi\left(\frac{V_{hub}}{0.4V_{ref}}\right)^{k}\right) \tag{2.2}$$

$$V_{ave} = C\sqrt{\frac{\pi}{2}} \tag{2.3}$$

According to [International Electronical Commission, 2005] a weibull distribution can be used to describe the wind distribution over an extended period of time. Normal the shape factor k is set to 2 and the wind condition at the site is set to Class I where $V_{ref} = 50m/s$. In Figure 2.1 the distribution is showed for three different mean wind classes:

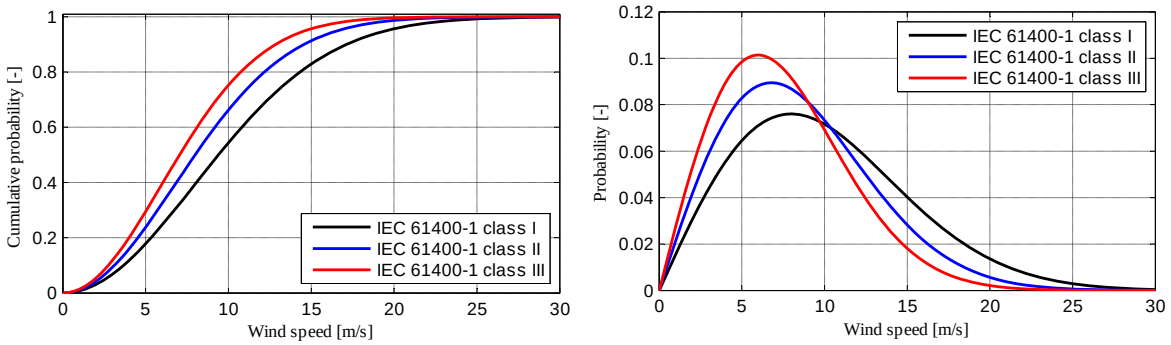

Figure 2.1: Wind distribution for class I, II and III [Henrik S. Toft, 2011].

When windfields are simulated and broken down to 10 minute intervals and then distributed by a weibull distribution, cycles larger than 10 minutes are neglected. This means that not all cycles the wind turbine will experience is counted. This problem is dealt with in [Larsen, G. C. and Thomsen, K , 1996] where a algorithm formulated to take this into account. An alternative algorithm, inspired by this, is also proposed. Both are implemented in Chapter 6, and their impact on the reliability of the wind turbine is analysed.

Fatigue

3

In this chapter a description of the SN-curves will be given along with the uncertanties connected to life time predictions and reliability calculations.

3.1 Introduction

In general, fatigue calculations are associated with large uncertainties. This is due to the fact that structural failure is a complex interaction between load, time and environment, where environmental loads can be caused by temperature or corrosion. Loads may vary from monotonous to a complete variable load (as for example wind or wave on a wind turbine) and be uniaxial or multiaxial. The time over which a structure is subjected to a load can vary from centuries, like for bridges or buildings, down to hours or even seconds.
Making life time predictions of steel structures will always be connected with a great amount of uncertainty. One way of describing fatigue strength is by an SN- or Wöhler-curve. An SN-curve is defined by the number of cycles until failure at a given stress range. The SN-curve can be expressed by Equation (3.1)

$$N = K S^{-m} \tag{3.1}$$

On a logarithmic scale Equation (3.1) shows a linear dependence between the stress range and the number of cycles to failure as seen in Equation (3.2).

$$\log(N) = \log(K) - m \log(S) \tag{3.2}$$

where

N	Number of cycles [-]
S	Stress range [MPa]
K	Material constant [-]
m	Wöhler exponent [-]

Figure 3.1 shows a plot of a bilinear SN-curve with a cut off limit on a logaritmic scale. The bilinear curve is the most common used for steel and has been proven by fatigue tests, which will be further investigated in the section below.

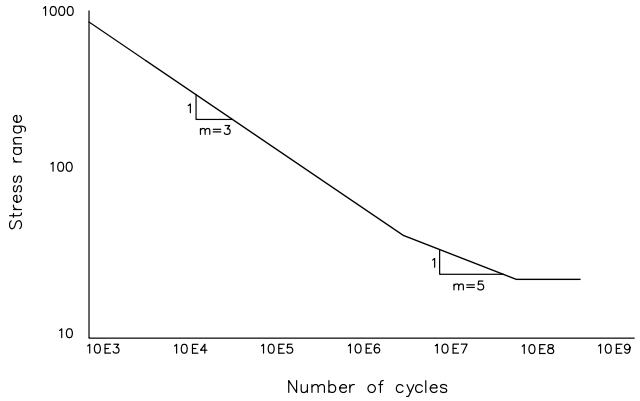

Figure 3.1: Example of an SN-curve.

The first part of the curve describes the linear part. This curve is the most conservative, since it predicts no smaller damage accumulation from the small stress ranges. The second part have a slope of $m = 5$ and is less conservative for the small stresses.

3.2 Uncertainties

The uncertainty of SN-curves can be divided into two groups: a physical uncertainty and statistical uncertainty. The physical uncertainty comes from locally imperfections on the surface of the material. These imperfections are associated with local stress concentrations, that for loads well under the yield limit can cause local plastic deformation because the stresses here can exceed the yield limit. When there is a cyclic loading the yield limit can be exceeded for each load cycle leading to a crack initiation and crack propagation phase, which eventually will cause a failure.

Equation (3.1) is based on a number of tests and that makes it affected by a statistical uncertainty. There is only one way to reduce this uncertainty, and that is by making more tests. But fatigue tests is both time consuming and can be very expensive.
One way of illustrating the uncertainties is by a reliability analysis of a component. In [Det Norske Veritas, 2010] an example of a calculated lifetime with mean SN data and design SN data shows the difference when the design SN-curve is defined as the mean minus two times the standard deviation. See Figure 3.2

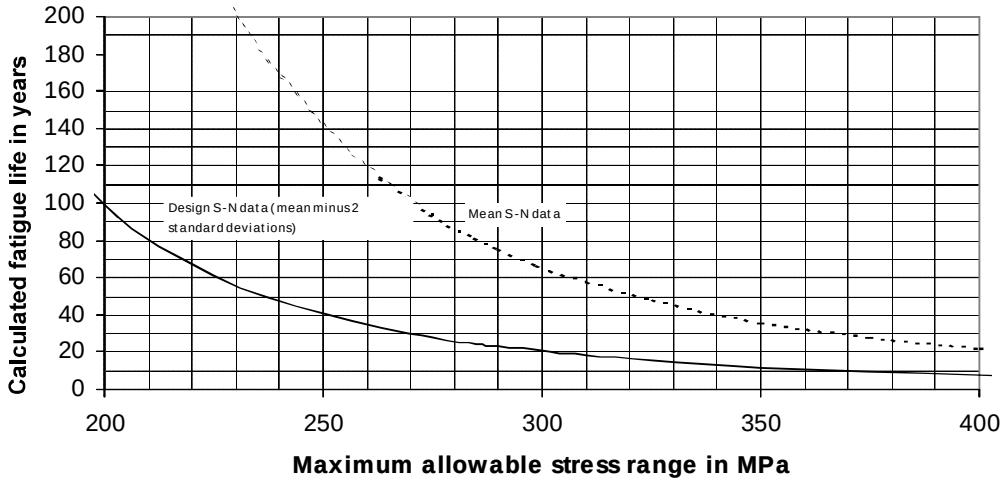

Figure 3.2: The influence of scatter shown by mean and design SN data in lifetime calculations. [Det Norske Veritas, 2010]

3.3 Fatigue Tests

SN-curves are made by fitting experimental data by linear regression. In Eurocode 3 the SN-curves are divided into different categories specified by their strength at 2 million cycles. The connection chosen to design is categorised as a load carrying welded constructional detail 3 with detail category $\Delta\sigma_c$ of 36 MPa, see Table 8.5 in [Eurocode 1993-1-9, 2005].
As explained in the previous section there are some uncertainties regarding fatigue life estimations. In this section the uncertainties regarding the scatter and amount of tests will be evaluated.
Six different tests will be used to examine the uncertainties. The first two test seres are made in the laboratory at Aalborg University and the last four are from the background document to Eurocode 3. Finally a seventh is assembled by combining all 6 test series, treating them as one, to investigate the influence of the standard deviation. The seven tests are listed in Table 3.1.

Test nr.	Reference
Test 1	Aaborg University
Test 2	Aaborg University
Test 3	LCW 10
Test 4	LCW 30
Test 5	1_1_q
Test 6	1_1_r
Test 7	All combined

Table 3.1: The seven tests investigated.

In Table 3.2 is the results from a fatigue test performed in laboratory at Aalborg University [J. U. Andersen, R. D. Brandstrup, 2003].

Stress range [MPa]	Number of cycles until failure [-]
45.22	2057708
57.55	995783
54.30	1089816
67.59	535911
87.98	268067
100.29	227872
112.07	115163
128.87	75237
136.93	41956
174.85	18766

Table 3.2: Results from test 1.

To obtain the parameters log(K) and m, least square method is used to get the best fit. Along with the least square fit the regression parameter R^2 is calculated to see how well the curve describe the data points.
With log(K) and m it is possible to compute log(N) values with the given stress ranges from test 1. The residuals can then be calculated by Equation (3.3)

$$y_{res} = log(N) - y_{fit} \tag{3.3}$$

where

y_{res}	residual values
y_{fit}	Fittet log(N) values by least square

R^2 is then found from Equation (3.4)

$$R^2 = 1 - \frac{S_{\text{y}_{res}}}{S_{\text{total}}} \tag{3.4}$$

$$S_{yres} = \sum_{i=1}^{n} y_{res}^2 \tag{3.5}$$

$$S_{total} = (n-1)\text{var}(log(N)) \tag{3.6}$$

where

n	Number of data points
$S_{\text{y}_{res}}$	sum of squared residuals
S_{total}	total sum of squares of log(N)
var(log(N))	Variance of log(N)

With R^2 it is possible to determine how many percent the fitted curve describe of the data points. The values of R^2 is listed in Table 3.3.
Due to scatter around the fitted curve it is quite difficult to predict the life time of a structure submitted to cyclic loading, as shown in Figure 3.2.
Several tests has formed the basis for the design SN-curves in [Eurocode 1993-1-9, 2005], where a reference value

for the stress level at $2 \cdot 10^6$ cycles defines the different curves. On Figure 3.3 Test 1 is plotted along with the fitted curve.

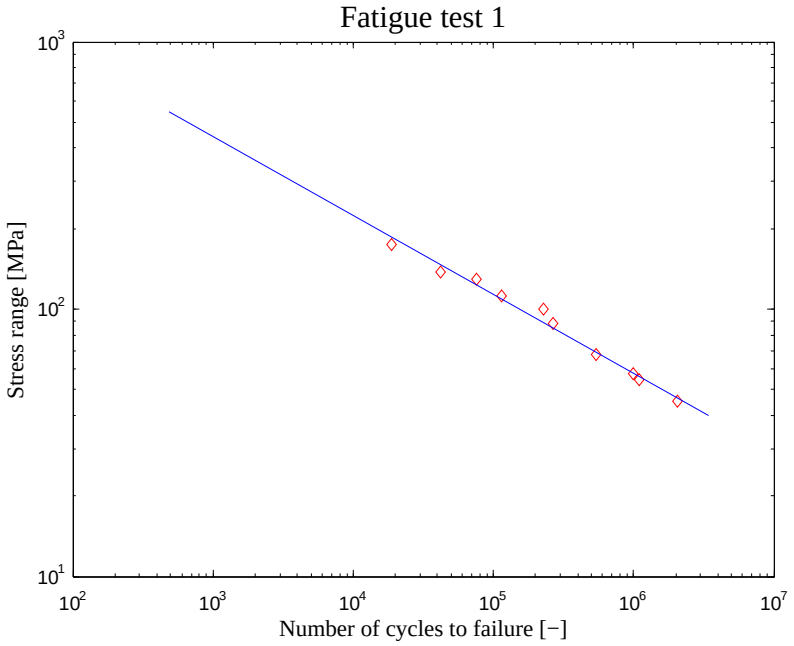

Figure 3.3: Test results from fatigue test 1

In Section 3.2, the uncertainties leading to the scatter of the fitted curve is described. One way of describing the scatter is to add an extra term to Equation (3.7):

$$\log(N) = \log(K) - m\log(S) + \varepsilon \tag{3.7}$$

where

ε	The lack of fit [MPa]

ε models the lack of fit and is assumed normal distributed with a mean value zero and a standard deviation of σ_ε. The standard deviation σ_ε describe the physical uncertainty whereas $\sigma_{\log(K)}$ and $\sigma_{\sigma_\varepsilon}$ describes the statistical uncertainties.
The parameters $\sigma_{\log(K)}$ and $\sigma_{\sigma_\varepsilon}$ can be found using the maximum likelihood method. From (3.7) the following model can be computed:

$$y = \alpha_0 + \alpha_1 x_1 + \varepsilon \tag{3.8}$$

where

y	log(N)
x_1	log(S)
α_0	regression parameter
α_1	regression parameter
ε	residual

The residual ε is assumed normal distributed with mean $\mu = 0$ and a standard deviation σ_ε. With n observations avalible the likelihood function can then be written:

$$L(\alpha_0, \alpha_1, \sigma_\varepsilon) = \prod_{i=1}^{n} P(y_i = \alpha_0, \alpha_1, \varepsilon) \tag{3.9}$$

Because ε is assumed to be normal distributed the likelihood function can be rewritten to:

$$L(\alpha_0, \alpha_1, \sigma_\varepsilon) = \prod_{i=1}^{n} \frac{1}{\sqrt{2\pi\sigma_\varepsilon}} \exp\left(-\frac{1}{2}\left(\frac{y_i - \alpha_0 + \alpha_1 x_{1i}}{\sigma_\varepsilon}\right)\right)^2 \tag{3.10}$$

The product form of the function in Equation (3.10) is difficult to differentiate. By making use of the fact that the logarithm of a variate must have its maximum at the same place as the maximum of the variate, Equation (3.10) can be rewritten to Equation (3.11)

$$\ln L(\alpha_0, \alpha_1, \sigma_\varepsilon) = -n\ln\left(\sqrt{2\pi\sigma_\varepsilon}\right) - \sum_{i=1}^{n} \frac{1}{2}\left(\frac{y_i - \alpha_0 + \alpha_1 x_{i1}}{\sigma_\varepsilon}\right)^2 \tag{3.11}$$

Equation (3.11) can then be optimized to find the maximum and thereby the best fitted parameters. This is done by using the nonlinear solver NLPQL.
In Table 3.3 the estimated parameters for SN-curves for the seven different test series are listed.

Test	Number of tests	m	$\log(K)$	σ_ε	$\sigma_{\log(K)}$	$\sigma_{\sigma_\varepsilon}$	R^2
Test 1	10	-3.376	11.940	0.079	0.03312	0.00178	0.98
Test 2	10	-3.080	11.162	0.130	0.04144	0.00440	0.95
Test 3	27	-2.999	12.245	0.218	0.04225	0.00465	0.85
Test 4	48	-2.103	9.775	0.374	0.07680	0.00671	0.66
Test 5	18	-3.294	11.743	0.169	0.04226	0.00192	0.95
Test 6	19	-3.132	11.640	0.212	0.04958	0.00592	0.93
Test 7	132	-2.166	9.898	0.453	0.16850	0.00510	0.58

Table 3.3: Fitted parameters by maximum likelihood.

From this Table, it is worth noticing Test 3 and 4. Test 3 is a very well performed test series, with relatively small scatter, whereas Test 4 is poorly graded, due to the including of 3 steel classes. The significance of this will be analysed in Chapter 8.

Characteristic SN-curves

4

In this chapter three different methods for calculating the characteristic SN-curves will be presented and compared. Six different tests from the previus chapter is used and finally the influence of scatter will be discussed.

4.1 Introduction

When using standard design SN-curves found in e.g. [Eurocode 1993-1-9, 2005] to calculate the fatigue strength of a welded joint, the SN-curves are subjected to some conservative choices. This is partly because the SN-curves are used in a variety of connections and used in many situations. The SN-curves in [Eurocode 1993-1-9, 2005] are made from a series of different tests with a constant amplitude, see Figure 4.1. Here it can be seen that different test series yields different slopes and are subject to some scatter. The tests can be found in the background documentation to Eurocode 3 [G. Sedlacek et al., 2002].
The tests used to calculate the characteristic SN-curves are listed in Table 4.1.

Test nr.	Reference	Fabrication
Test 1	Aaborg University	Submerged Arc Welding
Test 2	Aaborg University	Manual arc welding
Test 3	LCW 10	Manual arc welding, run off tabs removed by machining
Test 4	LCW 30	Manual arc welding, no machining
Test 5	1_1_q	MIG welded
Test 6	1_1_r	TIG welded
Test 7	All combined	-

Table 4.1: The seven tests investigated.

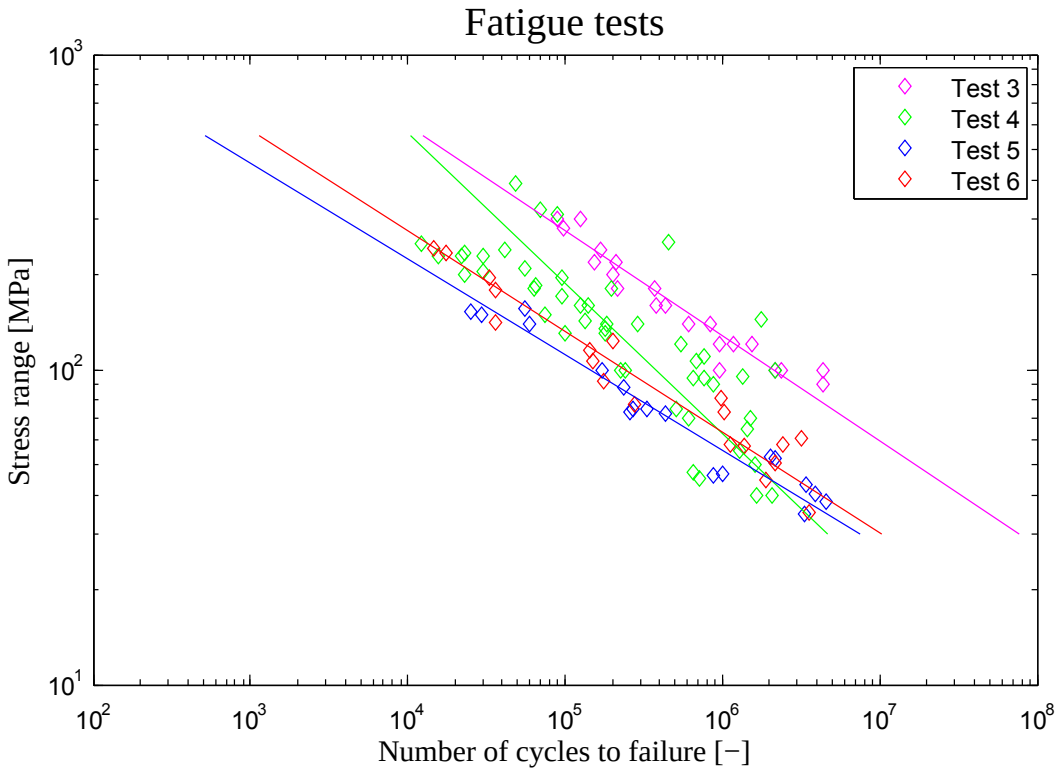

Figure 4.1: Test series from [G. Sedlacek et al., 2002].

With the test results it is now possible to calculate characteristic SN-curves to make safe estimation on the fatigue strength. There are several ways of constructing characteristic SN-curves. In Table 4.2 are three different approaches listed.

Document	Design criteria
Eurocode 3	75% confidence interval of 95% probability of survival for log(N)
Background for EC 3	95% lower confidence on log(N)
DNV-RP-C203	mean minus two standard deviations

Table 4.2: Characteristic SN-curves from different papers.

In Chapter 3 the welded joint in the wind turbine tower are classified as a load carrying weld joint. In [Eurocode 1993-1-9, 2005] Table 8.5 these are specified by 12 construction detail categories. The joint is classified to have a detail category of 36 MPa. In Appendix **??** the data for the four tests, plus two extra made at the laboratory at Aalborg University, are listed. In the following sections the theory for the three different approaches are described and an example with Test 1 is calculated.

4.2 Characteristic SN-curve by Background Documentation to Eurocode 3

In the Background documentation to Eurocode 3, the characteristic SN-curve are found from a 95% lower confidenceinterval on log(N). First a linear regression is made by least square method to determine the regression

parameters to Equation (3.2). This equation is rewritten to:

$$Y = b_0 + b_1 X \tag{4.1}$$

where

b_0	Regression coefficient
b_1	Regression coefficient

The vectors Y and X contains the values y_i and x_i where the following notation is used:

$$\begin{aligned} y_i &= \log(N) \\ x_i &= \log(S) \end{aligned} \tag{4.2}$$

The two unknown regression coefficients b_0 and b_1 are found from least square method. They are be found from following Equation (4.3) and (4.4) [Bilal M. Ayyub et al., 1997].

$$b_1 = \frac{\sum_{i=1}^{n} x_i y_i - \frac{1}{n}\sum_{i=1}^{n} x_i \sum_{i=1}^{n} y_i}{\sum_{i=1}^{n} x_i^2 - \frac{1}{n}\left(\sum_{i=1}^{n} x_i\right)^2} \tag{4.3}$$

$$b_0 = \bar{Y} - b_1 \bar{X} \tag{4.4}$$

In the equations above $\bar{Y}$ and $\bar{X}$ express the mean values of Y and X. With the regression parameters found, the standard error of estimate can be calculated which is used to find the confidence interval. Mathematically, the standard error of estimate equals the standard deviation of the errors, and has the same units as Y [Bilal M. Ayyub et al., 1997].

$$S_e = \sqrt{\frac{1}{\nu}\sum_{i=1}^{n} (\hat{y} - y_i)^2} \tag{4.5}$$

In Equation (4.5) ν states the number of degrees of freedom which equals the sample size minus the unknowns. Because there in equation (4.1) are two unknowns the degrees of freedom becomes ν = n-2.
The confidence interval evaluates the accuracy of a single point $\hat{y}$ for a given value x_0. To evaluate the characteristic SN-curve a lower 95 % confidence interval is used, corresponding to a level of significance at $\alpha = 0.05$.
The estimated value of Y, which is denoted by $\hat{y}$, is given by:

$$\hat{y} = \bar{Y} + b_1(x_0 - \bar{X}) \tag{4.6}$$

The point of interest, x_0, is the point in which the detail category is defined. In Eurocode 3 this is set to 2.000.000 cycles.

$$x_0 = \frac{b_1 - \log(2.000.000)}{b_0} \tag{4.7}$$

Then the confidence interval can be determined by Equaion (4.8).

$$\hat{y} - S_e t_{\alpha/2} \sqrt{1 + \frac{2}{n} + \frac{(x_f - \bar{X})^2}{\sum_{i=1}^{n} (x_i - \bar{X})^2}} \tag{4.8}$$

4.2.1 Example of the Characteristic SN-curve Calculated by the Background Documentaion to Eurocode 3

Test 1 made in the laboratory at Aalborg University, consist of a series of 10 experiments on a load carrying weld with constant amplitude, see Table 3.2. The following notation is used from Equation (4.2):

$$\begin{aligned} y_i &= \log(N) \\ x_i &= \log(S) \end{aligned} \tag{4.9}$$

The linear regression with least square is done with:

$$b_1 = \frac{\sum_{i=1}^{n} x_i y_i - \frac{1}{n}\sum_{i=1}^{n} x_i \sum_{i=1}^{n} y_i}{\sum_{i=1}^{n} x_i^2 - \frac{1}{n}\left(\sum_{i=1}^{n} x_i\right)^2} \;=\; 11.940 \tag{4.10}$$

and

$$b_0 = \bar{Y} - b_1 \bar{X} \;=\; -3.376 \tag{4.11}$$

Then the standard error of estimate can be calculated by

$$S_e = \sqrt{\frac{1}{\nu}\sum_{i=1}^{n} (\hat{y} - y_i)^2} \;=\; 0.0887 \tag{4.12}$$

The mean curve can now be found to

$$\log(N) = 11.940 - 3.376 \log(S) \tag{4.13}$$

The characteristic SN-curve can now be found from the results from Test 1 by a 95% lower confidence interval for log(N) with a level of significance $\alpha = 0.05$ and a $t_{\alpha/2} = 2.306$.

$$\hat{y} - S_e t_{\alpha/2} \sqrt{1 + \frac{2}{n} + \frac{(x_f - \bar{X})^2}{\sum_{i=1}^{n} (x_i - \bar{X})^2}}$$

$$\hat{y} - 0.2352 \tag{4.14}$$

Then the characteristic SN-cuve can be written:

$$\log(N) = 11.940 - 3.376 \log(S) - 0.2352$$

$$\log(N) = 11.7048 - 3.376 \log(S) \tag{4.15}$$

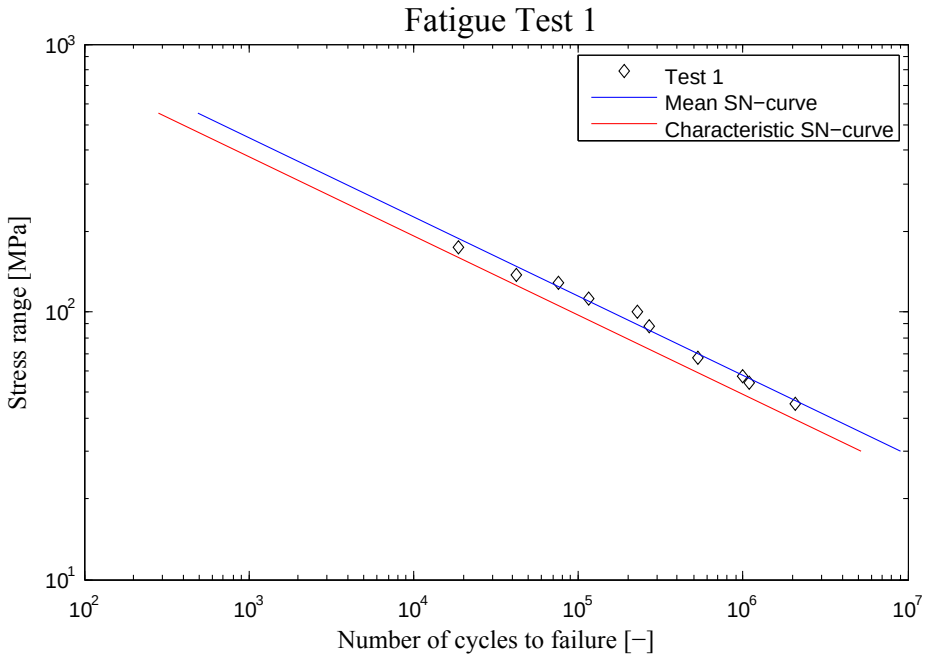

Figure 4.2: Characteristic SN-curve with a 90% confidence interval.

Figure 4.2 shows how the characteristic SN-curve is parallel translated from the mean curve with the lower confidence. The detail category is found at N = 2.000.000 cycles to:

$$\log(2.000.000) = 11.7048 - 3.376\log(S)$$

$$\log(S) = \frac{11.7048 - \log(2.000.000)}{3.76} = 39.878\text{MPa} \tag{4.16}$$

4.2.2 Example of the Characteristic SN-curve Calculated by the Background Documentaion to Eurocode 3 with a Fixed Slope of $m = 3$

In Eurocode 3 the curves have a fixed slope at m = -3. This affects the regression parameters and confidence interval for the characteristic SN-curve. With a fixed slope the regression parameter becomes:

$$b_0 = -3 \tag{4.17}$$

$$b_1 = \bar{Y} - b_0\bar{X} = 11.2091 \tag{4.18}$$

The standard error of estimate becomes

$$S_e = \sqrt{\frac{1}{\nu}\sum_{i=1}^{n}(\hat{y} - y_i)^2} = 0.1179 \tag{4.19}$$

The characteristic SN-curve with a fixed slope can now be found from the results from Test 1 by a 95% lower confidence interval for log(N) with a level of significance $\alpha = 0.05$ and a $t_{\alpha/2} = 2.306$.

$$\hat{y} - S_e t_{\alpha/2} \sqrt{1 + \frac{2}{n} + \frac{(x_f - \bar{X})^2}{\sum_{i=1}^{n} (x_i - \bar{X})^2}}$$

$$\hat{y} - 0.3196 \tag{4.20}$$

Then the characteristic SN-cuve can be written:

$$\log(N) = 11.2091 - 3\log(S) - 0.3196$$

$$\log(N) = 10.8895 - 3\log(S) \tag{4.21}$$

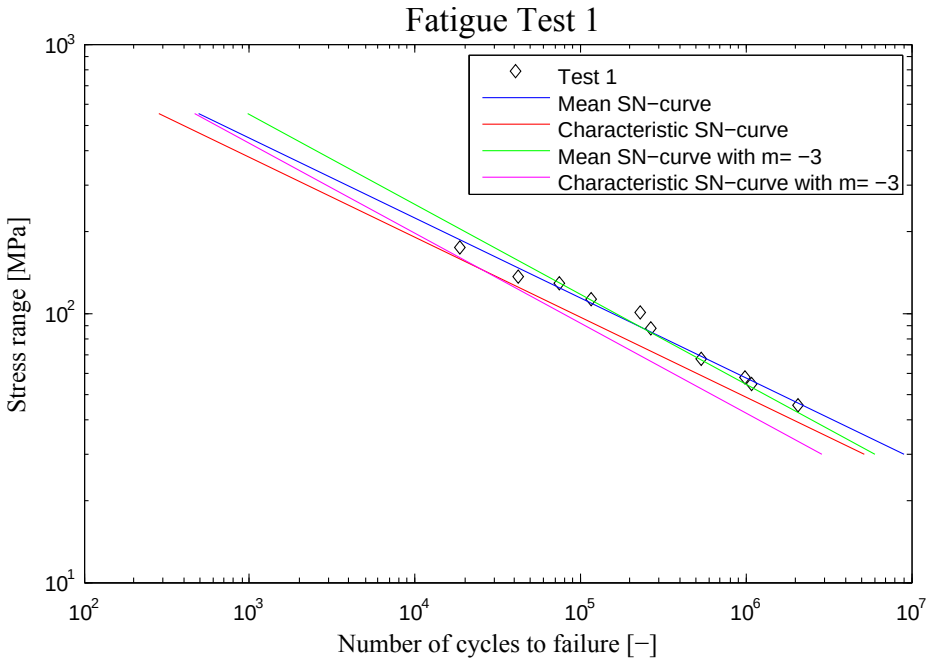

Figure 4.3: Characteristic SN-curve with a 90% confidence interval for a fixed slope of m = 3.

Plottet together with Figure 4.2 it can be seen that with a fixed slope of m = -3 the standard error of estimate increases and thereby the confidence interval gets wider. This means that from approximate 20000 cycles the fatigue strength will get more conservative.
The detail category is found for a fixed slope at $N = 2 \cdot 10^6$ cycles to:

$$log(2.000.000) = 10.8895 - 3\,log(S)$$

$$log(S) = \frac{10.8895 - log(2.000.000)}{3} = 33.84\text{MPa} \tag{4.22}$$

In Table 4.3 values for all seven tests are listed.

Test	Dof	$t_{\alpha/2}$	S_e	$\hat{y}$ - *	m	log(K)	Detail kategory
Test 1	8	2.306	0.089	0.2352	-3.376	11.7048	39.88
Test 2	8	2.306	0.146	0.4136	-3.080	10.7484	27.80
Test 3	25	2.060	0.226	0.4820	-2.999	11.7630	66.24
Test 4	46	2.014	0.382	0.8050	-2.103	8.9704	18.60
Test 5	16	2.120	0.179	0.3988	-3.294	11.3442	33.96
Test 6	17	2.110	0.225	0.4994	-3.132	11.1406	35.10
Test 7	130	1.978	0.4563	0.9141	-2.166	8.9842	17.34
Test 1	8	2.306	0.118	0.3196	-3	10.8895	33.84
Test 2	8	2.306	0.147	0.4196	-3	10.5847	26.78
Test 3	25	2.060	0.226	0.4820	-3	11.7649	66.27
Test 4	46	2.014	0.445	0.9200	-3	10.7513	30.44
Test 5	16	2.120	0.191	0.4273	-3	10.7729	30.95
Test 6	17	2.110	0.227	0.5062	-3	10.8756	33.49
Test 7	130	1.978	0.500	0.9975	-3	10.5999	27.10

Table 4.3: Values for characteristisk SN-curves by Background Documentation to EC 3.

4.3 Characteristic SN-curve by Eurocode 3

Because SN-curves are based on test results they are subjected to a statistical uncertainty. To take this statistical uncertainty into concideration, in Eurocode 3 the characteristic SN-cuve is calculated by a 75% confidence interval of 95% probability of survival for log(N). The test are described by equation (4.23)

$$\log(N) = \log(K) - m\log(S) \tag{4.23}$$

$$\log(K) = \log(N) + m\log(S) \tag{4.24}$$

The characteristic value $x_{i,k}$ is determined as a 5% quantile for a distribution function $F_X(x)$, where X is modelled as a stokastic variable (corresponding to an infinite numer of results). In the case where a limited number of results are avalible, the following metohod is used.[J. D. Sørensen, 2003]
For each test a number of results n are avalible. In the following these will be described by $x_1, x_2, ..., x_i$ and is assumed to be from a homogeneous population. The characteristic value x_k is determined as a lower end point in a 75% confidence $q = 0.75$ interval for the quantile value $p = 0.05$.
X is assumed to be normal distributed with with a mean μ and a standard deviation σ, hence is the characteristic value x_k defined as the p-quantile value:

$$x_k = \mu + u_p\sigma \tag{4.25}$$

where

$$u_p = \Phi^-1(p) \tag{4.26}$$

Φ	Standard Normal Distribution

Because the test results is assumed normal distributed and the standard deviation is unknown, the following is used

to determine the characteristic value x_k. The mean μ and varians s^2 is calcualted by:

$$\bar{x} = \frac{1}{n}\sum_{i=1}^{n} x_i \tag{4.27}$$

$$s^2 = \frac{1}{n-1}\sum_{i=1}^{n} (x_i - \bar{x})^2 \tag{4.28}$$

$\bar{x}$ i an outcome of the stochastic variable $\bar{X}$ which is normal distributed with mean μ_X and standard deviation $\sigma/\sqrt{n}$. $(n-1)s^2/\sigma^2$ is an outcome of the stochastic variable $(n-1)S^2/\sigma^2$ which is χ^2 distributed with $n-1$ degrees of freedom.[H. S. Toft, 2009]
Then on basis of the test results $\bar{x}$ and s it is possible to estimate the characteristic value x_k:

$$x_{sk} = \bar{x} - k_s s \tag{4.29}$$

x_{sk} is an outcome of the stochastic variable X_{ks}. The factor k_s is determined in a way such that the probability for X_{ks} less than x_{sk} is at least $q = 0.75$. So x_{sk} is on the safe side on X_{ks} [H. S. Toft, 2009].

$$P(X_{sk} \leq x_k) = P(\bar{X} - k_s S \leq \mu + u_p \sigma \tag{4.30}$$

$$= P\left(\frac{\frac{\bar{X}-\mu}{\sigma/\sqrt{n}} - u_p\sqrt{n}}{S/\sigma} \leq k_s\sqrt{n}\right) \tag{4.31}$$

$$= P\left(T\left(n, -u_p\sqrt{n}\right) \leq k_s\sqrt{n}\right) \geq q \tag{4.32}$$

Where $T(n, -u_p\sqrt{n})$ is a noncentral t-distribution with $n-1$ degrees of freedom and the noncentrality parameter $\lambda = -u_p\sqrt{n}$. For given values of p, n and q, k_s can be determined. Figure 4.4 shows k_s dependence of n.

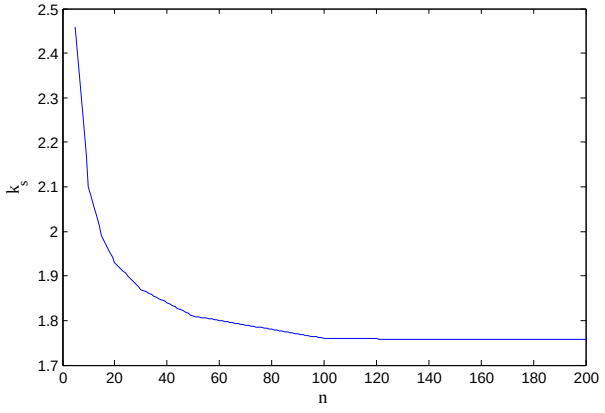

Figure 4.4: k_s dependency of number of test resultes.

Before the characteristic SN-curve can be calculated a linear regression must be performed. This is done by Least Square Method where the parameter m are found.

4.3.1 Example of the Characteristic SN-curve Calculated by the Eurocode 3

The characteristic SN-curve from Eurocode 3 made by a 75% confidence interval of 95% probability of survival for $\log(N)$ will in this example be calculated for Test 1. Test 1 made in the laboratory at Aalborg University, consist

of a series of 10 experiments on a load carrying weld with constant amplitude, see table 3.2.
The characteristic curve is made from the model:

$$\hat{x} = \log(K) = log(N) + m\log(S) \tag{4.33}$$

From the linear regression the parameter m is found to -3.376. Then the μ and s can be calculated by (4.27) and (4.28).

$$\bar{x} = \frac{1}{n}\sum_{i=1}^{n} x_i \; = \; 11.9406 \tag{4.34}$$

$$s^2 = \frac{1}{n-1}\sum_{i=1}^{n}(x_i - \bar{x})^2 \; = \; 0.007 \; \Rightarrow s \; = \; 0.0836 \tag{4.35}$$

From figure 4.4 is can be seen that with n=10 the k_s can be found to 2.10. Then the characteristic value $x_k s$ from equation (4.36) can be evaluated.

$$x_{sk} = \bar{x} - k_s s \; = 11.9406 - 2.10 \cdot \; 0.0836 \; = \; 11.7650 \tag{4.36}$$

With x_{ks} and equation (4.23) can the characteristic SN-curve now be formulated as:

$$\log(N) = 11.7650 - 3.376\log(S) \tag{4.37}$$

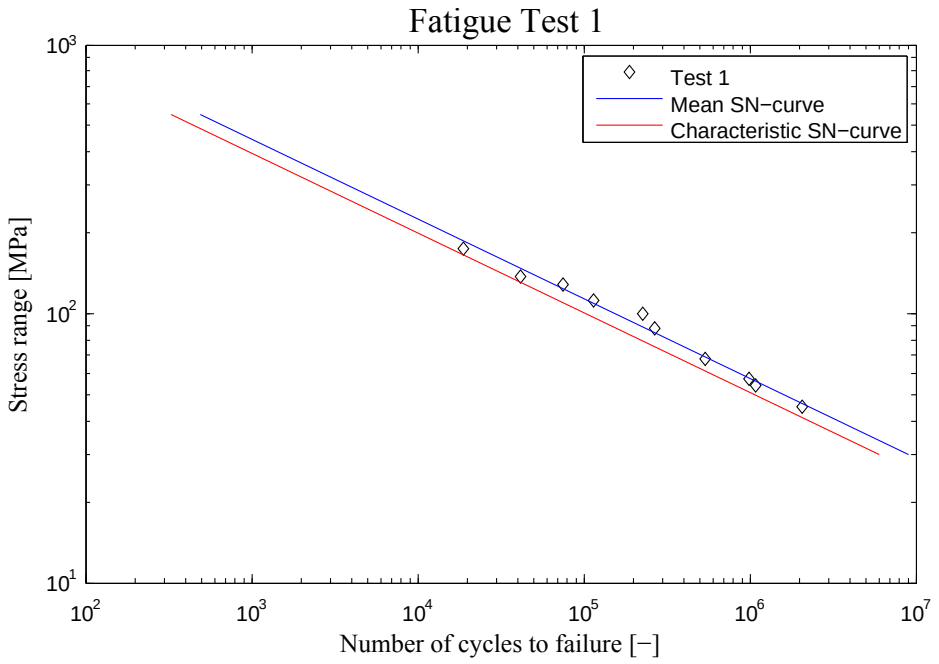

Figure 4.5: Characteristic SN-curve with a 75% confidence interval of 95% probability of survival for log(N).

On figure 4.5 it is seen as in figure 4.2 how the characteristic curve is parallel translated from the mean SN-curve. The detail category is found at N = 2.000.000 cycles to:

$$\log(2.000.000) = 11.7650 - 3.376\log(S)$$

$$\log(S) = \frac{11.7650 - \log(2.000.000)}{3.376} = 41.55\text{MPa} \tag{4.38}$$

4.3.2 Example of the Characteristic SN-curve Calculated by the Eurocode 3 with a Fixed Slope of m = -3

With the characteristic curve made from the model:

$$\hat{x} = \log(K) = \log(N) + 3\log(S) \tag{4.39}$$

The parameter m is set to -3. Then from equation (4.27) and (4.28) the mean μ and standard deviation s can be calculated by:

$$\bar{x} = \frac{1}{n}\sum_{i=1}^{n} x_i \;=\; 11.2091 \tag{4.40}$$

$$s^2 = \frac{1}{n-1}\sum_{i=1}^{n} (x_i - \bar{x})^2 \;=\; 0.0124 \Rightarrow s \;=\; 0.1112 \tag{4.41}$$

From figure 4.4 is can be seen that with n=10 the k_s can be found to 2.10. Then the characteristic value x_{ks} from equation (4.36) can be evaluated.

$$x_{sk} = \bar{x} - k_s s \;= 11.2091 - 2.10 \cdot\; 0.1112 \;=\; 10.976 \tag{4.42}$$

With x_{ks} and equation (4.23) can the characteristic SN-curve now be formulated as:

$$\log(N) = 10.976 - 3\log(S) \tag{4.43}$$

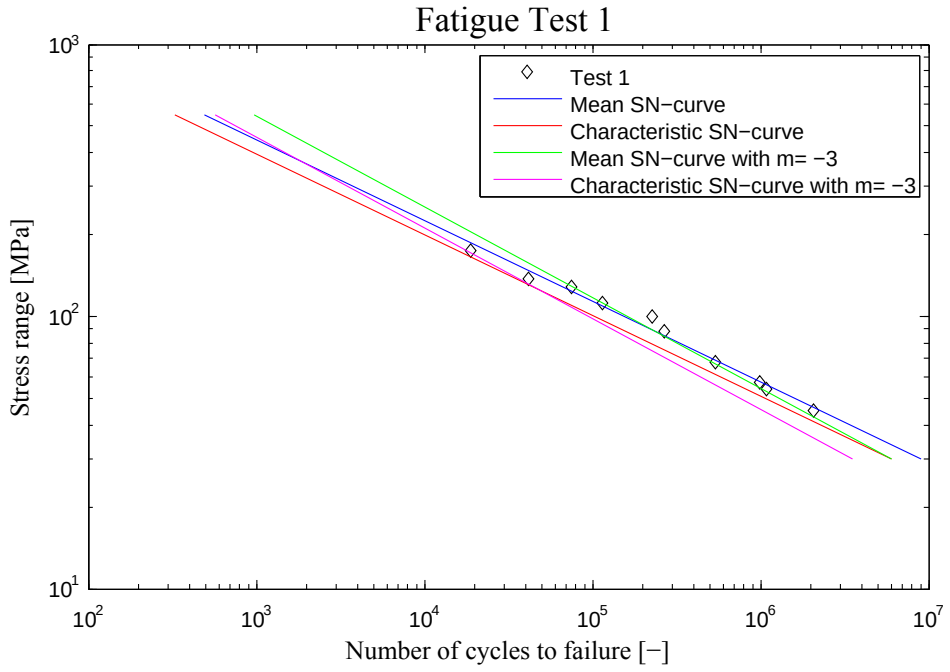

Figure 4.6: Characteristic SN-curve with a 75% confidence interval of 95% probability of survival for log(N) for a fixed slope of m = -3.

As for figure 4.3 it can be seen that when the slope is fixed to m = -3 the curve fits the test results poorly. This results in a more conservative fatige strength for N < 30.000 cycles.

The detail category is found at N = 2.000.000 cycles to:

$$\log(2000000) = 10.976 - 3\log(S)$$

$$\log(S) = \frac{10.976 - \log(2000000)}{3} = 36.16\text{MPa} \tag{4.44}$$

In table 4.4 all values for the characteristic SN-curves calculated from Eurocode 3 listed.

Test	log(K)	m	Detail kategory
Test 1	11.765	-3.376	41.55
Test 2	10.874	-3.080	30.53
Test 3	11.826	-2.999	69.52
Test 4	9.089	-2.103	21.17
Test 5	11.403	-3.294	35.39
Test 6	11.216	-3.132	37.10
Test 7	9.100	-2.166	19.60
Test 1	10.976	-3	36.16
Test 2	10.714	-3	29.58
Test 3	11.872	-3	69.54
Test 4	10.838	-3	33.40
Test 5	10.953	-3	32.53
Test 6	10.828	-3	35.54
Test 7	10.721	-3	29.74

Table 4.4: Values for characteristisk SN-curves by Eurocode 3.

4.4 Characteristic SN-curve by DNV-RP-C203

In [Det Norske Veritas, 2010] the characteristic SN-curve is defined as the mean minus two times the standard deviation for the relevant test data. The SN-curves are thus assosiated with a 97.7 probability of survival.
From the test results a given stress range, S, correspond to a numer of cycles, N, until failure. A linear regresssion with least square method is then used to describe the linear relationship between $\log(S)$ and $\log(N)$. With the linear relationship it is possible to calculate the estimated parameter for $\log(\hat{N})$. Then the residual ε can be found by:

$$\varepsilon = \log(\hat{N}) - \log(N) \tag{4.45}$$

The residual ε is assumed to be normal distributed with mean $\mu = 0$ and a standard deviation σ. From equation (4.46) it is possible to determine the standard deviation and therby the characteristic SN-curve:

$$S = \sqrt{\frac{1}{n-1}\sum_{i=1}^{n}\varepsilon_i^2} \tag{4.46}$$

4.4.1 Example of the Characteristic SN-curve Calculated by DNV-RP-C203

From the linear regression the mean SN-curve is found to:

$$\log(N) = 11.940 - 3.376\log(S) \tag{4.47}$$

From equation (4.46) the standard deviation on the residual ε is found to:

$$S = \sqrt{\frac{1}{n-1}\sum_{i=1}^{n}\varepsilon_i^2} = 0.0836 \tag{4.48}$$

Then the characteristic SN-curve becomes:

$$\log(N) = 11.940 - 3.376\log(S) - 2 \cdot 0.0836 \Rightarrow \tag{4.49}$$

$$\log(N) = 11.7728 - 3.376\log(S) \tag{4.50}$$

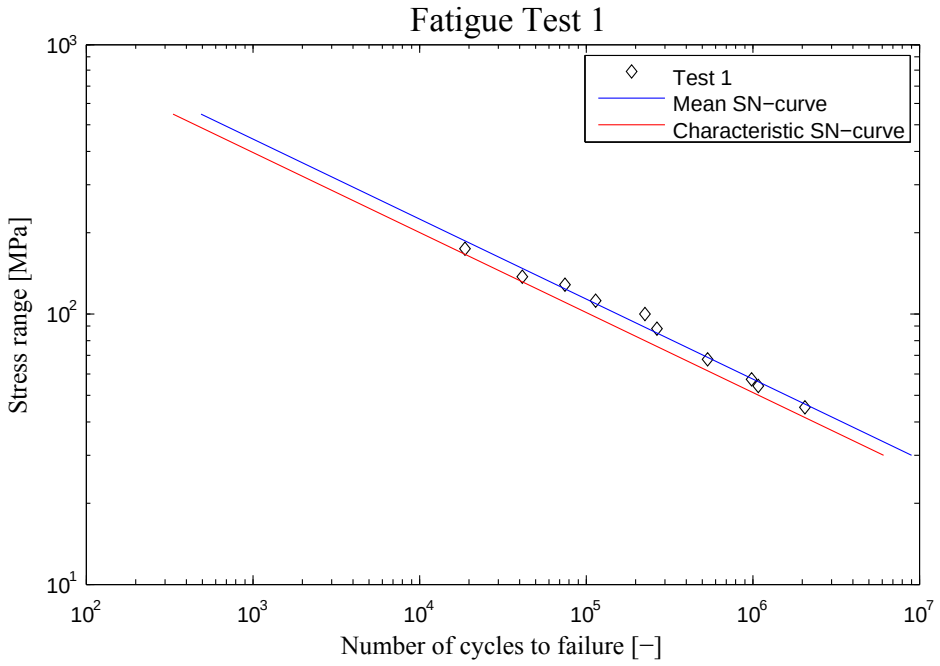

Figure 4.7: Characteristic SN-curve with mean minus two times the standard deviation.

The detail category is found at N = 2.000.000 cycles to:

$$\log(2.000.000) = 11.7728 - 3.376\log(S)$$

$$\log(S) = \frac{11.7728 - \log(2.000.000)}{3.376} = 36.45\text{MPa} \tag{4.51}$$

In table 4.5 are the values for the characteristic SN-curves calculated by DNV-RP-C203 listed.

Test	log(K)	m	Detail category
Test 1	11.7728	-3.376	41.77
Test 2	10.8876	-3.080	30.85
Test 3	11.8010	-2.999	68.20
Test 4	9.0185	-2.103	19.61
Test 5	11.3952	-3.294	35.19
Test 6	11.2035	-3.132	36.76
Test 7	8.9891	-2.166	17.43
Test 1	10.9867	-3	36.47
Test 2	10.7280	-3	29.90
Test 3	11.8029	-3	68.23
Test 4	10.7914	-3	31.39
Test 5	10.8292	-3	32.31
Test 6	10.9403	-3	35.19
Test 7	10.6011	-3	27.12

Table 4.5: Values for characteristic SN-curves by DNV-RP-C203.

4.5 Comments to the Characteristic SN-curves

In the previous sections three different methods for obtaining a characteristic SN-curve is described. In this section Test 3, Test 4 and Test 7 will be further commented and the results will be presented with the design method found in the background document to Eurocode 3. Test 7 will also be used to compare the three different methods for calcualting the characteristic SN-curve to see what influence this have.

As stated in chapter 3 calculating the fatigue strength of a cyclic loaded welded joint is quite difficult. From the test results in section 4.2, 4.3 and 4.4 is seen that for some tests the agreement with [Eurocode 1993-1-9, 2005] is not totally clear. Two test in particularly are of interest. If we look at Test 3 the slope of the curve is found to $m = 2.999$ which is in good accordance with [Eurocode 1993-1-9, 2005], whereas for Test 4 the slope is found to $m = 2.103$. In Figure 4.8 Test 3 and Test 4 is plotted, for both a free slope and slope rotated to $m = 3$, together with the design curve from [Eurocode 1993-1-9, 2005].

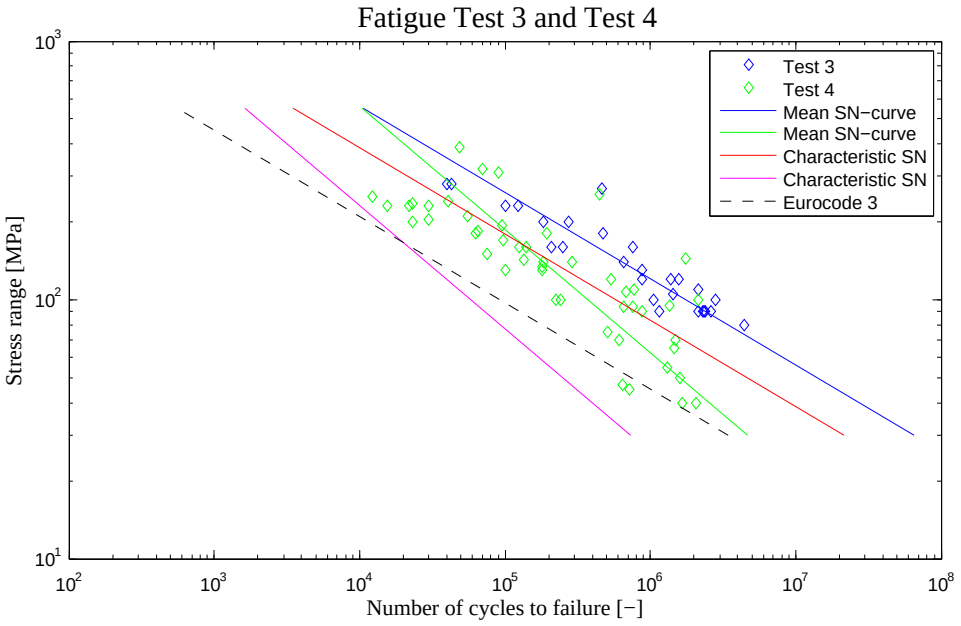

(a)

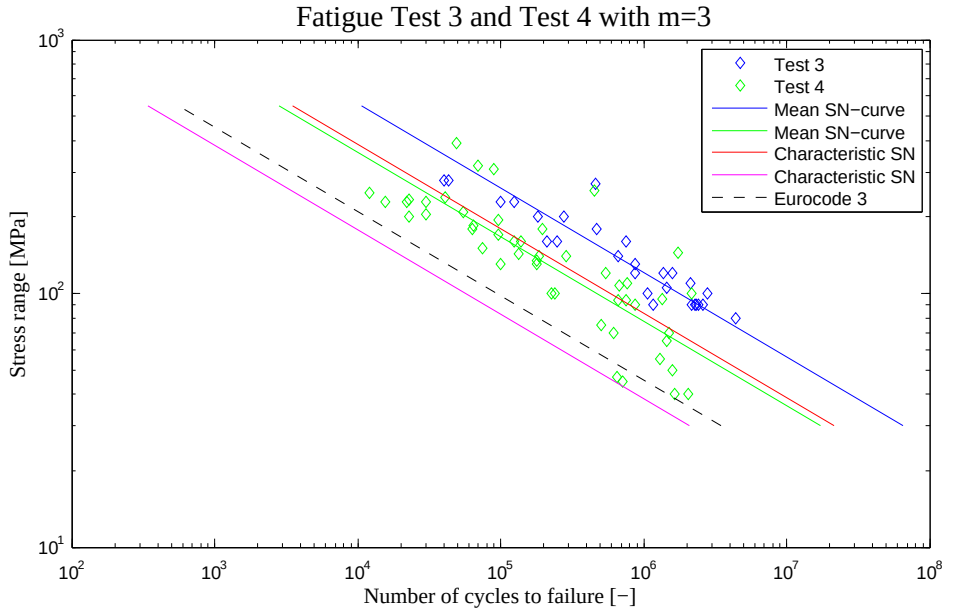

(b)

Figure 4.8: Test 3 and Test 4 with mean and characteristic curves calculated from the Background Documentation to Eurocode 3.

Figure 4.8(a) shows the best fitted curves and 4.8(b) the best fitted curves with a fixed slope of $m = 3$. Test 3 shows the very small difference there is between a free and fixed slope, whereas for Test 4 the difference is more significant. The scatter around the mean curves is seen to be larger for Test 4 than for Test 3, and if we look at the results from table table 4.3, the standard error of estimate becomes larger for Test 4. When the curves are rotated to a fixed slope of $m = 3$ the alignment of Test 3 is very small and therefore results in very small changes. For Test 4 the rotation results in the standard error of estimate increases and the the confidence interval therefor gets wider.

But because the slope is changed from $m = 2.103$ to $m = 3$ the estimate on the fatigue strength becomes slightly less conservative.
The impact on the stress range at 2.000.000 cycles gives the same tendency. In table 4.6 the stress range for which the joint will fail at 2.000.000 is listed.

Test	m = free [MPa]	m = 3 [MPa]
Test 3	66.24	66.27
Test 4	18.60	30.44

Table 4.6: Stress ranges at 2.000.000 cycles for which the test will fail.

The difference between Test 3 and Test 4 can be explained by the fact that Test 3 have had some post treatment. The fabrication of Test 3 and Test 4 are made with manual arc welding, but as seen from table 4.1 there is a significant difference between the the two tests. Test 3 had run off tabs removed by machining which could help the test results to get more homogeneous and thereby reduce the level scatter.
Another difference is that Test 4 consist of three different steel grades HT 60, HT 70 and HT 80. This could also contribute to the larger scatter in Test 4.
Test 7 is made from combining the two tests made in the laboratory at Aalborg University and the four tests related to load carrying welded joint from [G. Sedlacek et al., 2002], with detail category 36, and should therefore be representative to compare to the design SN-curve from Eurocode 1993-1-9 [2005].

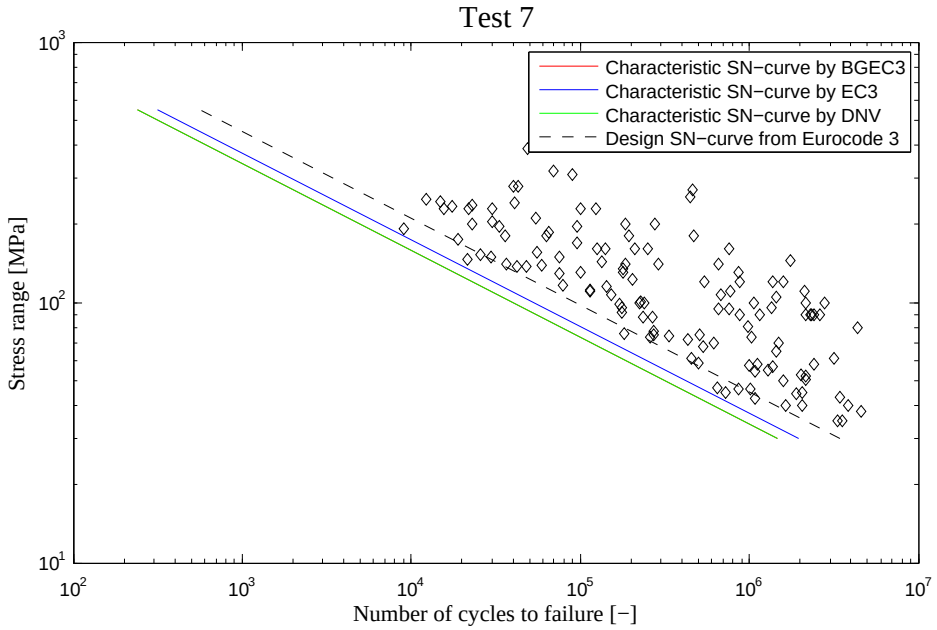

Figure 4.9: Characteristic SN-curves compared to the design SN-curve from Eurocode 3.

In Figure 4.9 the characteristic SN-curves calculated by the methods listed in Table 4.2 is plotted with a fixed slope of $m = 3$ along with the design SN-curve from [Eurocode 1993-1-9, 2005]. With data from all tests added together the scatter of course increase and the standard deviation for the residual to the best fitted line also increase. This is seen from both table 3.3 and Table 4.3.
It is interesting to see that the methods from [Det Norske Veritas, 2010] and [G. Sedlacek et al., 2002] agrees very well with a detail category of 27.10 MPa and 27.12 MPa for $2 \cdot 10^6$ cycles. The method from [Eurocode 1993-1-9,

2005] is slightly less conservative with a detail category of 29.74 MPa. But still all three methods are under the design value of 36 MPa.
It can be concluded that there are a lot of things influencing the fatigue strength. All data comes from experiments, and when making a test-specimen it is impossible to make two of the same kind. Both the human factor and imperfections in the metal will give different results each time a test is conducted. There fore a lot of time consuming tests are necessary to make a fairly accurate estimate of the life time for a cyclic affected joint.
Then there are different ways of making the characteristic SN-curve to adjust for these uncertainties. The three different approaches were analysed and the general tendency is that [Det Norske Veritas, 2010] and [G. Sedlacek et al., 2002] agrees very well for tests with high standard deviation. Where as the method from [Eurocode 1993-1-9, 2005] is slightly less conservative. For low standard deviations the methods from [Eurocode 1993-1-9, 2005] and [Det Norske Veritas, 2010] agrees. Which method to use is in the end up to the owner of the given structure.
In Table 4.7 the detail category for $N = 2.000.000$ cycles are summarised. In chapter 8 the probability of failure is calculated and the effect of the different SN-curves will be discussed.

Test	Background Documentation to EC 3	Eurocode 3	DNV-RP-C203
Test 1	39.88	41.55	41.77
Test 2	27.80	30.53	30.85
Test 3	66.24	69.52	68.20
Test 4	18.60	21.17	19.61
Test 5	33.96	35.39	35.19
Test 6	35.10	37.10	36.76
Test 7	17.34	19.60	17.43
	m = 3		
Test 1	33.84	36.16	36.47
Test 2	26.78	29.58	29.90
Test 3	66.27	69.54	68.23
Test 4	30.44	33.40	31.39
Test 5	30.95	32.53	32.31
Test 6	33.49	35.54	35.19
Test 7	27.10	29.74	27.12

Table 4.7: Values for characteristic SN-curves by DNV-RP-C203.

Code based Fatigue Design, EC

5

In this Chapter, the design according to [Eurocode 1993-1-9, 2005] is implemented, and a reliability analysis is performed.

5.1 Introduction

The design will be made with respect to a design parameter, z, for the response series of the wind turbine modelled in FAST. A reliability analysis will be performed of the connection, as a result of the code based determination of z, to check whether the required reliability is reached. The reliability analysis will be made by two approaches: 1) a Monte Carlo realisation of stochastic variables modelling the uncertainties of key parameters, and 2) an implementation of First Order Reliability Method, based on the same stochastic model. The SN-curves used for design and reliability analysis are from [Eurocode 1993-1-9, 2005], but the requirements to the reliability index is found implicit from DNV-RP-C203, since no one is defined in Eurocode 3.

As previously discussed, the design codes for fatigue damage is based on the correlation between the magnitude and number of stress cycles, called SN-curves. [Eurocode 1993-1-9, 2005] propose three types of SN-curves: Linear, Bilinear and Bilinear with cut-off. A series of bilinear SN-curves with cut-off can be seen at Figure 5.1

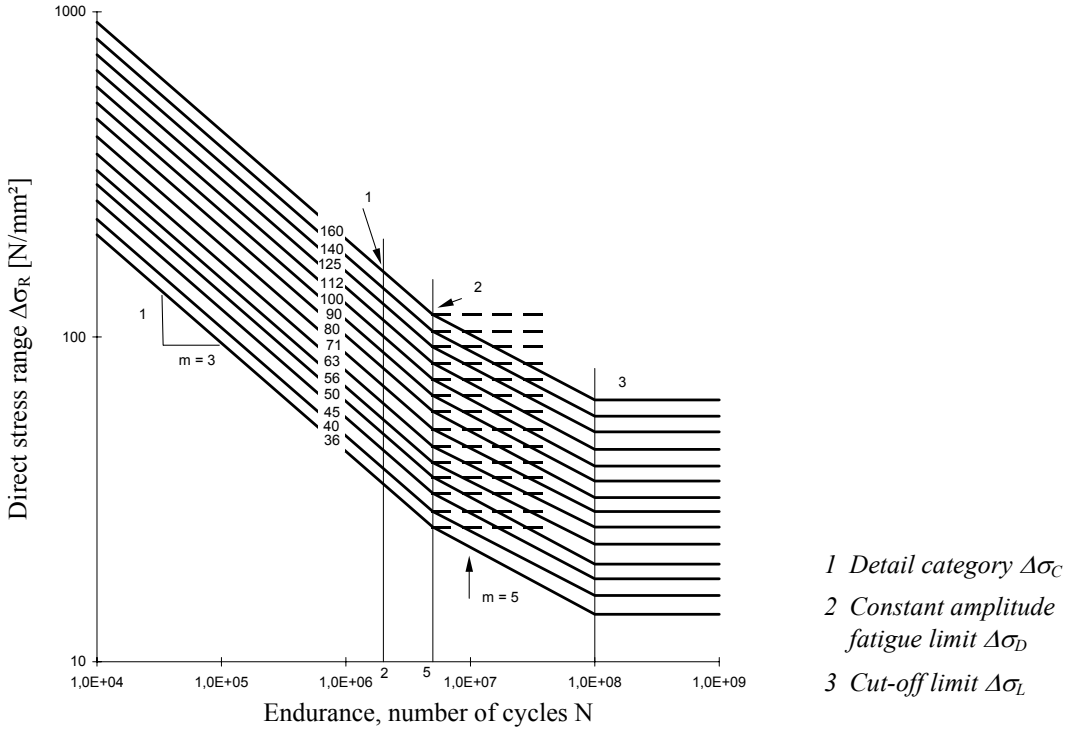

Figure 5.1: Bilinear SN-curves with cut-off, [Eurocode 1993-1-9, 2005]

For a linear case, only the slope of the first part of the curve is used. For a bilinear case, the last part of the curve, the cut-off, is ignored. The connection in the wind tower that is to be designed is considered detail category 36, see Figure 5.1. The data defining this curve is therefore used for the further design, see Table 5.1.

Parameter	Value
$\log K_{linear}$	10.9699 [-]
$\log K_{bilinear}$	13.8172 [-]
m_{linear}	3 [-]
$m_{bilinear}$	5 [-]
N_D	$5x10^6$
N_L	$1x10^8$

Table 5.1: Data defining the SN-curve.

The fatigue life may be calculated by the use of linear accumulation of damage summation implemented by Palmgren-Miner rule, (5.1).

$$D = \sum_{i=1}^{k} \frac{n_i}{N(S_i)} = \sum_{i=1}^{k} \frac{n_i}{K \cdot S_i^{-m}} \geq 1 \tag{5.1}$$

where

n_i	Number of occuring stress cycles [MPa]
$N(S_i)$	Number of stress cycles to failure with constant stress S_i [-]

Based on the SN-curve described by the data in Table 5.1 and the Palmgren-Miner rule in equation (5.1), a design equation, G, can be formulated to optimise the design parameter. The design parameter is used in a limit state

equation to calculate the accumulated reliability index. An acceptable accumulated reliability index for a lifetime of 20 years, β_{acc}, is implicit accepted according to [Det Norske Veritas, 2010], as the values in Table 5.2.

Parameter	Value
FDF_{linear}	1.5 [-]
$FDF_{bilinear}$	2.0 [-]
$\beta_{acc,linear}$	1.6 [-]
$\beta_{acc,bilinear}$	2.6 [-]

Table 5.2: Stochastic parameters.

The index of FDF and β in Table 5.2denotes which SN-curve has been used as design curve. The FDF implements the partial safety factors, γ_f and γ_m for the load and strength respectively. This implementation can be seen in Equation (5.2)

$$FDF = (\gamma_f \gamma_m)^m \tag{5.2}$$

With the SN-curve described in Table 5.1 and the FDF defined in Table 5.2, the design equations can be assembled.

5.2 Design Equation

The design equations are assembled for the three SN-curves: linear, bilinear and bilinear w. cut-off. These can be seen as Equation (5.3), (5.4) and (5.5)

$$G = 1 - \sum_{i=1}^{n_U} \sum_{j=1}^{n_Q} FDF\, T_L n_{ij} \sum_{s_j} \frac{s_j^{m_1}}{K_1^C} = 0 \tag{5.3}$$

$$G = 1 - \sum_{i=1}^{n_U} \sum_{j=1}^{n_Q} FDF\, T_L n_{ij} \left(\sum_{s_j \geq \Delta s_D} \frac{s_j^{m_1}}{K_1^C} + \sum_{s_D \geq \Delta s_i} \frac{s_j^{m_2}}{K_2^C} \right) = 0 \tag{5.4}$$

$$G = 1 - \sum_{i=1}^{n_U} \sum_{j=1}^{n_Q} FDF\, T_L n_{ij} \left(\sum_{s_j \geq \Delta s_D} \frac{s_j^{m_1}}{K_1^C} + \sum_{\Delta s_D \geq s_j \geq \Delta s_L} \frac{s_j^{m_2}}{K_2^C} \right) = 0 \tag{5.5}$$

where

G_i	Design equation
$\sum_{i=1}^{n_U}$	Summation of wind speeds [m/s]
$\sum_{j=1}^{n_Q}$	Summation of response [kNm]
T_L	Life time [years]
n_{ij}	Number of stress cycles per year, [-]
s_j	Stress ranges [MPa]
s_D	Constant amplitude fatigue limit [MPa]
s_L	Cut-off limit [MPa]
m_1	Wöhler exponent, linear part [-]
m_2	Wöhler exponent, bilinear part [-]
K_1^C	Material parameter characteristc, linear part [-]
K_2^C	Material parameter characteristc, bilinear part [-]
FDF	Fatigue design factor [-]

and where the stress ranges can be found by

$$s_j = \frac{Q_j}{z}(T/T_{ref})^{\alpha} \tag{5.6}$$

where

Q_j	Tower responce [kNm]
z	Resistance torque [m^3]
T	Thickness of specimen [mm]
T_{ref}	Reference thickness [mm]
α	Scale exponent [-]

The last part of Equation (5.6) takes thickness effects of the connection into consideration. The tower response is determined from the FAST simulations described in Chapter 2, and with the input data from Table 5.1 and the FDF defined in Table 5.2, the design parameter, z, can be found. Since the response from FAST is found as a moment, the design parameter z is chosen as a resistance torque, so stress ranges can be obtained by Equation (5.6). This is done for the three cases of SN-curves, and the results can be seen in Table 5.3

Parameter	Value	Percentage
z_{linear}	4209 [m^3]	100 %
$z_{bilinear}$	3115 [m^3]	74 %
$z_{bilinearw.cut-off}$	2967 [m^3]	70 %

Table 5.3: Stochastic parameters.

The reliability of the wind turbine is analysed with respect to these values, to check if an acceptable safety is reached.

5.3 Limit State Equation

With a design parameter found in section 5.2 the corresponding limit state equation can be assembled. As for the design equations, the limit state equations, g, are assembled for the three cases of SN-curves. These equation can be seen at Equation (5.7), (5.8) and (5.9) respectively.

$$g(t) = \Delta - \sum_{i=1}^{n_U}\sum_{j=1}^{n_Q} tn_{ij} \sum_{s_j} \frac{s_j^{m_1}}{K_1^C} = 0 \tag{5.7}$$

$$g(t) = \Delta - \sum_{i=1}^{n_U}\sum_{j=1}^{n_Q} tn_{ij} \left(\sum_{s_j \geq \Delta s_D} \frac{s_j^{m_1}}{K_1^C} + \sum_{s_D \geq \Delta s_j} \frac{s_j^{m_2}}{K_2^C} \right) = 0 \tag{5.8}$$

$$g(t) = \Delta - \sum_{i=1}^{n_U}\sum_{j=1}^{n_Q} tn_{ij} \left(\sum_{s_j \geq \Delta s_D} \frac{s_j^{m_1}}{K_1^C} + \sum_{\Delta s_D \geq s_j \geq \Delta s_L} \frac{s_j^{m_2}}{K_2^C} \right) = 0 \tag{5.9}$$

where the stress ranges are found by Equation (5.10)

$$s_j = X_W X_{SCF} \frac{Q_j}{z}(T/T_{ref})^{\alpha} \tag{5.10}$$

and where

g	Limit state equation, [-]
Δ	Stochastic variable, Miners rule, [-]
t	Time, [year]
X_W	Stochastic variable, wind load [-]
X_{SCF}	Stochastic variable, stress concentration factor [-]
α	Scale exponent [-]

The stochastic variables used for the modelling of the limit state equations are defined in Table 5.4.

Parameter	Distribution	Mean value, μ_i	Standard deviation, σ_i
Miners rule, X_Δ	Lognormal	1	0.3
Wind load, X_w	Lognormal	1	0.2
Stress calculation, X_{SCF}	Lognormal	1	0.1
Material parameter, linear part, K_{lin}	Normal	11.3699	0.2
Material parameter, bilinear part, K_{bilin}	Normal	14.2172	0.2

Table 5.4: Stochastic parameters.

The *K*-parameters are modelled fully correlated, using the characteristic values from [Eurocode 1993-1-9, 2005], added two times the standard deviation. The standard deviation is assumed to be 0.2 for both K-parameters. Miners rule, wind load and stress concentration are modelled as fully uncorrelated. The distribution, mean value and standard deviations of the three remaining parameters are obtained from [J. D. Sørensen, 2011] and by recommendation of supervisor of the thesis, Prof. John Dalsgaard Sørensen.

5.4 Reliability Analysis

As mentioned in the beginning of this chapter, two methods are proposed to determine the accumulated reliability index of the wind turbine. First a Monte Carlo simulation is performed with 100.000 simulations, and secondly First Order Reliability Method is used. The Monte Carlo simulation and FORM are both calcualted to validade each other and to check the results are converging.

5.4.1 Monte Carlo Simulation

The Monte Carlo simulation is made for each case of SN-curve, with their corresponding z-parameter, see Table 5.3 The independent stochastic variables defined in Table 8.2 are realised by Equation (5.11)

$$X_i = \mu_i + \sigma_i x_i \tag{5.11}$$

where

X_i	Outcome of stochastic variable
u_i	Outcome of a standard normal- or lognormal distribution [-]

With the uncertainties modelled by the stochastic variables and realised by Equation (5.11), the Monte Carlo simulation can be made. The resulting accumulated reliability index can be seen at Figure 5.2.

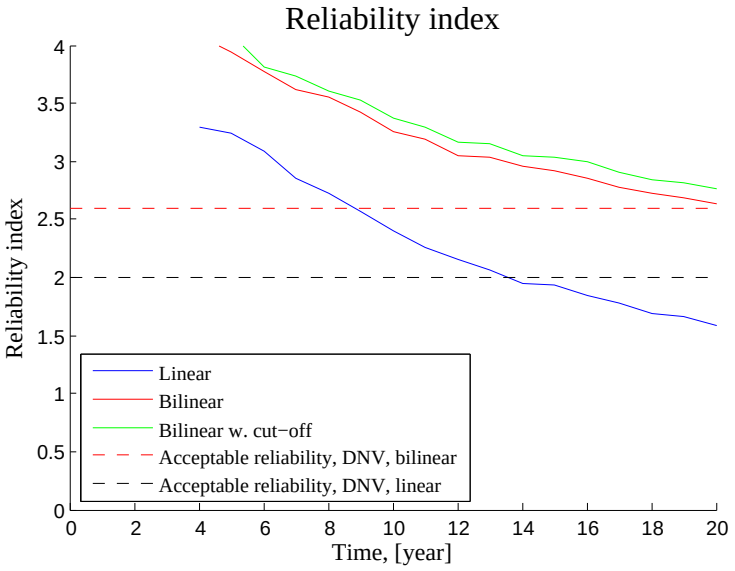

Figure 5.2: Accumulated reliability index for linear, bilinear, and bilinear w. cut-off.

It can be seen that the reliability index does not provide usable results the early years. This is due to no failures occurring, resulting in a limit value of the reliability of 36.69. This pin-points the shortcomings of Monte Carlo simulations, but can be helped with more simulations. The highest reliability index from 100.000 simulations is caused by only one failure, giving a β value of 4.26. A higher number of simulations could have been run, but since the scope of interest is the accumulated reliability index for a lifetime of 20 year, this is not deemed necessary. A visualisation of the simulations are made at Figure 5.3 for the design using a bilinear SN-curve with cut-off.

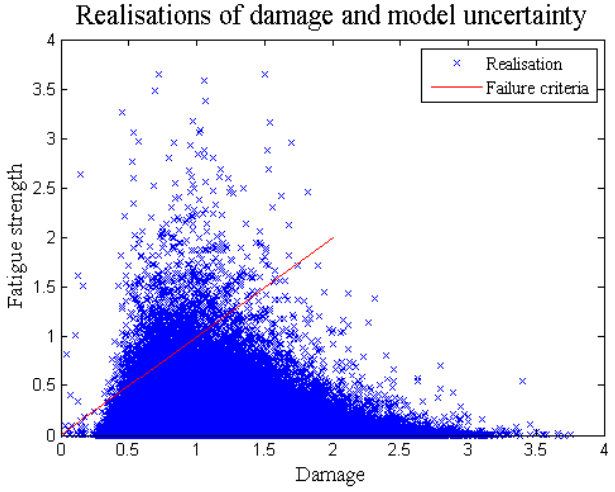

Figure 5.3: Outcome of limit state equations, bilinear with cut-off.

The Figure shows the realisation of the resulting damage and the model uncertainties regarding Miners rule. It can be see that the uncertainty regarding miners rule is dominant with the shape of lognormal distribution seen around the damage. The failure criteria based on Equation (5.9) is marked, showing the failures to the left side of this line. Results can be seen in Table 5.5

5.4.2 First Order Reliability Method

Another method to determine the reliability index is by the First Order Reliability Method, further on abbreviated to FORM. Here the reliability index is calculated by normalising the stochastic variables from X-space into the normalized U-space [J. D. Sørensen, 2004]. The stochastic variables are denoted X_i and assumed to be independent. Normal distributed variables are nomalized by Equation (5.12)

$$U_i = \frac{X_i - \mu_{X_i}}{\sigma_{X_i}} \qquad i = 1,2,...,n \tag{5.12}$$

The limit state function defined by the equations (5.8), (5.9) and (5.10) consist of the stochastic variables listed in Table 5.4. The lognormal distributed stochatic variables can transformed to the U-space by following definition:

$$\Phi(U_i) = F_{X_i}(X_i) \tag{5.13}$$

where F_{X_i} is the distribution function for X_i. Given a realisation $\mathbf{u}$ of $\mathbf{U}$ a realisation $\mathbf{x}$ of $\mathbf{X}$ can be determined by:

$$x_1 = F_{X_i}^{-1}(\Phi(u_i)) \tag{5.14}$$

For a lognormally distributed variable X with expected value μ and standard deviation σ the distribution function is:

$$F_x(x) = \Phi\left(\frac{\ln x - \mu_L}{\sigma_L}\right) \tag{5.15}$$

where

$$\sigma_L = \sqrt{\ln\left(\frac{\sigma^2}{\mu} + 1\right)} \tag{5.16}$$

$$\mu_L = \ln\mu - \frac{1}{2}\sigma_L^2 \tag{5.17}$$

The transformation for a lognormal stochastic variable then becomes, [J. D. Sørensen, 2004]:

$$x = \exp(\sigma_L u + \mu_L) \tag{5.18}$$

With the stochastic variables transformed into the nomalized U-space the reliability index β can be found by the following iteration:

1. Guess $\mathbf{u}$ set i = 0

2. Calculate g($\mathbf{u}_i$)

3. Calculate ∇ g($\mathbf{u}_i$)

4. Calculate an improved guess of the β point using

   $\mathbf{u}_{i+1} = \nabla g(\mathbf{u}_i)\frac{\nabla g(\mathbf{u}_i)^T \mathbf{u}_i - g(\mathbf{u}_i)}{\nabla g(\mathbf{u}_i)^T - \nabla g(\mathbf{u}_i)}$

5. Calculate the corressponding reliability index

$$\beta_{i+1} = \sqrt{(\mathbf{u}_{i+1})^T \mathbf{u}_{i+1}}$$

6. If β convergence (β_{i+1} - $\beta_i \leq 10^{-3}$ the reliability index is found, else go back to step 2.

When convergence is achieved in step 6, the results at Figure 5.4 are found.

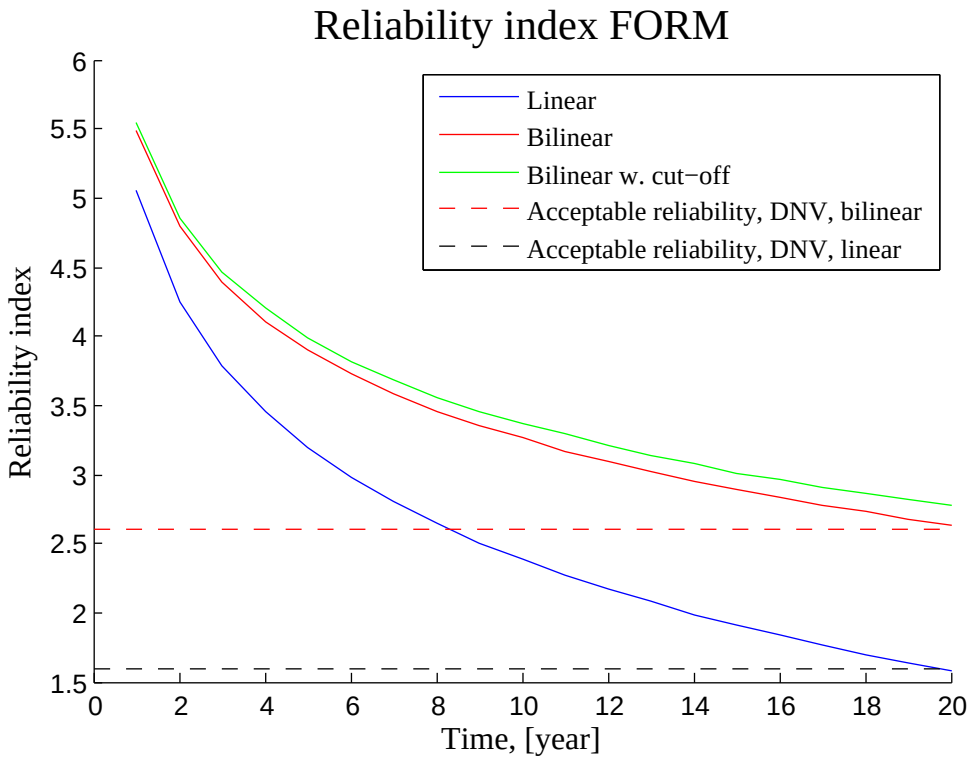

Figure 5.4: Accumulated reliability index for linear, bilinear, and bilinear w. cut-off, FORM.

As for the results obtained from the Monte Carlo simulations, a good correspondence with the code recommendations is achieved. In contradiction with the Monte Carlo method, no problems with small probabilities of failure is occurring when using FORM. The resulting accumulated reliability can be seen in Table 5.5 for both the Monte Carlo simulation and FORM.

Parameter	Reliability index, EC	Probability of failure
Linear	1.58	0.0571
Bilinear	2.63	0.0043
Bilinear w. cut-off	2.76	0.0029
Linear	1.58	0.0571
Bilinear	2.63	0.0043
Bilinear w. cut-off	2.77	0.0028

Table 5.5: Z-values for linear and bilinear SN-curves, obtained from Monte Carlo and FORM, for t = T_L.

The reliability is seen to correspond fairly well with the required, according to the code. For comparison, the code recommendations can be found in Table 5.2.

Low Cycle Fatigue Loads

6

In this Chapter, an extra load contribution, Low Cycle Fatigue Load, will be quantified. A reliability analysis is performed to analyse the impact of implementing this load.

6.1 Introduction

As explained in the Chapter 1, the SN-curves and the linear damage accumulation by Miners rule is the most common method to design for fatigue load cases. The loads applied are usually found from independent simulated wind series, of 10 minutes length. From this load, the response of the tower is found, also in independent 10 minute intervals. By assuming independency of the load series, the cycles with longer duration than 10 min. are neglected This topic has been treated in [Larsen, G. C. and Thomsen, K , 1996], in where a simple algorithm has been presented to include low cycle fatigue. The algorithm will be implemented for a wind turbine case, which will be shown in this chapter. Beside the theory described in [Larsen, G. C. and Thomsen, K , 1996], another method proposed by the authors of this project is presented. This method is inspired by [Larsen, G. C. and Thomsen, K , 1996]. The resulting increase in fatigue damage will be quantified for both methods, and due to this, an updated reliability of the wind turbine will be evaluated.

6.2 Design Equation

To include the Low cycle Fatigue contribution to the damage, the design equation (6.1) is used. This equation is for the case of a bilinear SN-curve, and the Low cycle Fatigue is included in the last part.

$$G = 1 - \sum_{i=1}^{n_U} \sum_{j=1}^{n_Q} FDF\, T_L n_{ij} \left(\sum_{s_j \geq \Delta s_C} \frac{s_j^{m_1}}{K_1^C} + \sum_{s_D \geq \Delta s_j} \frac{s_j^{m_2}}{K_2^C} \right) - \sum_{j=1}^{n_Q} T_L n_{0j} \left(\sum_{s_j \geq \Delta s_D} \frac{s_j^{m_1}}{K_1^C} + \sum_{s_D \geq \Delta s_j} \frac{s_j^{m_2}}{K_2^C} \right) = 0 \tag{6.1}$$

where

n_{0j}	Number of stress cycles, Low cycle Fatigue, [-]

To determine the impact on the accumulated damage, the design parameter, z, of wind turbine tower is designed with a bilinear SN-curve, without Low cycle Fatigue. This parameter is then kept constant for the other cases of SN-curves, to see the change in damage.

6.3 Low cycle fatigue RISØ

To include the extra contribution induced by the stress cycles from the low frequency loads, the theory in [Larsen, G. C. and Thomsen, K , 1996] is applied. This theory include an extra stress cycle when moving from a simulated

series with one mean value to another. The magnitude of this cycle is determined from the global max and min of each of the series. An example of the simulated series of response can be seen at Figure 6.1, where 5 series are shown.
Besides the simulated series of response, an order for them to appear in, is necessary. This is obtained by using the order of measurements from an offshore location. This data contains the mean wind speed over 30 min. from Horns Rev, over a period of 3 years. The order and frequency in which the wind speed changes in the measurements, is used for the series. For a given mean wind speed the time series in this 10-minute period is chosen randomly from the available 6 time series for that mean wind speed. An example of the final series of the tower response providing the low frequency cycles can be seen at Figure 6.1.

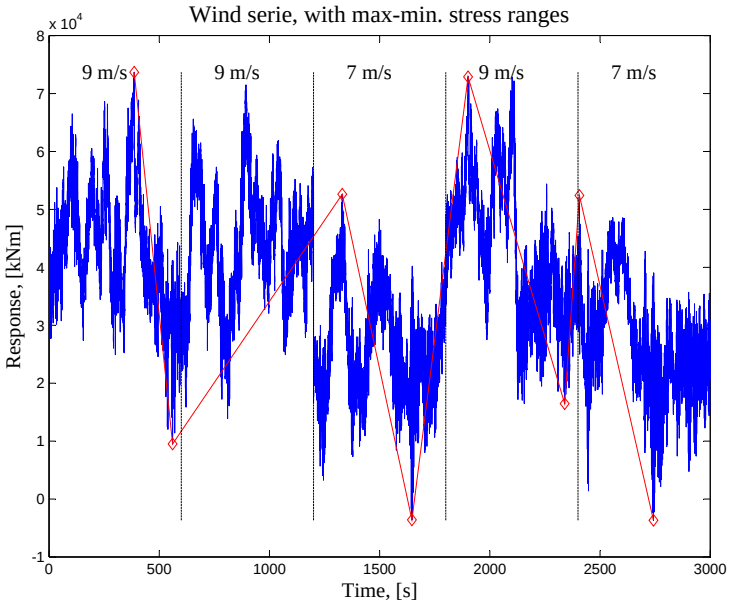

Figure 6.1: Response series of tower with low cycles marked red.

The red markings shows the cycles that are added by the LCF algorithm. As can be seen from Figure 6.1, the LCF is only included if a change in mean wind speed is happening. A histogram of the measurements with a fitted Weibull distribution can be seen in Appendix 11, to verify the data. By using the order from Horns Rev and the simulated response, a new series is obtained, for which the damage can be found. This is illustrated by Figure 6.2, which shows the extra yearly contribution to the load, due to LCF.

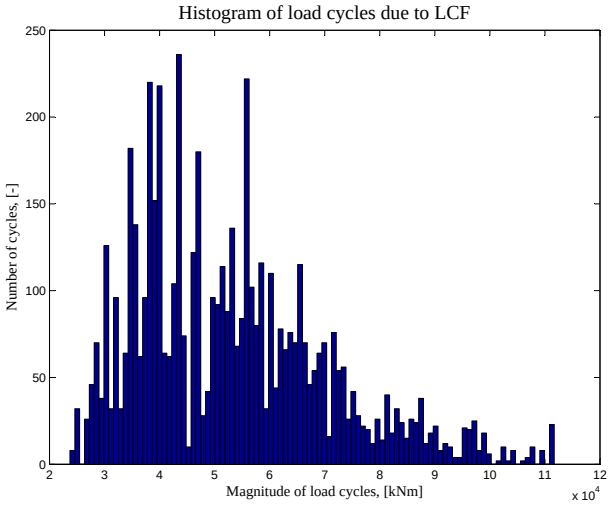

Figure 6.2: Histogram of yearly response series, due to low cycle fatigue.

The plot at Figure 6.2 can be seen to have a significantly scatter. This is due to the limited number of simulations made. Since only 6 series are produced for each mean wind speed, and the change in mean wind speed tends to change with one bin at the time, the possible outcome for the LCF contribution is somewhat limited. The resulting yearly load can be seen at Figure 6.3

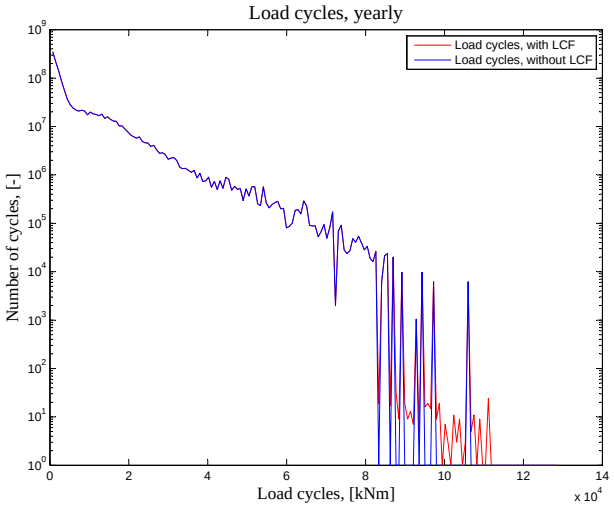

Figure 6.3: Histogram of yearly response series, with and without low cycle fatigue.

As can be seen at Figure 6.3, the number of cycles caused by LCF is rather small compared to the entire load. The magnitude of the load cycles is however among the largest ones occurring. The extra LCF load is applied to the case of a connection described by detail category 36, and a composite material.

6.3.1 Steel connection in tower

With the response series known, a rainflow counting and a damage summation with Miners rule is made, with and without the extra contribution, to determine the impact of the applied theory. The data for the used SN-curve can be seen in Table 6.1, where the z-parameter is fitted for a design with bi-linear SN-curve, without LCF included.

Parameter	Value
Detail category	36 [MPa]
m_{linear}	3
$m_{bi-linear}$	5
Bi-linear limit, cycles	5x10^6 [-]
Cut-off limit, cycles	1x10^8 [-]
Bi-linear limit, stress	26.5 [MPa]
Cut-off limit, stress	14.6 [MPa]
Design parameter, z, linear	4209 [m^3]
Design parameter, z, bilinear	3115 [m^3]
Design parameter, z, bilinear w. cut-off	2967 [m^3]

Table 6.1: Characteristics of SN-curve.

The results obtained can be seen in Table 6.2

Case	Linear	Bi-linear	Bi-linear w. cut-off
Without LCF	2.468	1.000	0.747
With LCF	2.485	1.019	0.766
Percentage increase	0.68%	1.90%	2.48%

Table 6.2: Damage to the tower.

The results correspond fairly well with [Larsen, G. C. and Thomsen, K , 1996], where increase in damage is found to be in the order of 1%, with Wöhler coefficients of 3 and 5. From the results it can be seen that the the impact on the damage is increasing with the use of bi-linear and cut-off SN-curves. This is as expected, since the low cycle fatigue loads in general are of a larger magnitude, and therefore does not get influenced by a cut-off for the lower stress ranges .

To investigate the importance of which detail category is used, the damage is found with and without LCF for three other cases. The detail categories chosen can be seen in Table 6.3, as well as the rest of the data describing the SN-curves. The z-parameter is determined for a bi-linear SN-curve, Equation (5.4), without LCF.

	Detail category		
Parameter	71 [MPa]	112 [MPa]	160 [MPa]
m_{linear}	3	3	3
$m_{bi-linear}$	5	5	5
Bi-linear limit, cycles	5x10^6 [-]	5x10^6 [-]	5x10^6 [-]
Cut-off limit, cycles	1x10^8 [-]	1x10^8 [-]	1x10^8 [-]
$\log K_{linear}$	11.8548 [-]	12.4487[-]	12.9134[-]
$\log K_{bi-linear}$	15.2920 [-]	16.2818[-]	17.0563[-]
Design parameter, z	1579 [m^3]	1001 [m^3]	701 [m^3]

Table 6.3: Characteristics of SN-curves.

Using the data in Table 6.3 and the load including LCF, the corresponding damage can be found. As for detail category 36, all three cases of SN-curves are used, both with and without LCF. The results can be seen in 6.4.

SN-curve	Linear	Bi-linear	Bi-linear w. cut-off
		Detail cat. 71	
Without LCF	2.470	1.000	0.835
With LCF	2.488	1.020	0.846
Percentage increase	0.19%	2.02%	1.31%
		Detail cat. 112	
Without LCF	2.469	1.000	0.748
With LCF	2.487	1.020	0.767
Percentage increase	0.16%	2.01%	1.18%
		Detail cat. 160	
Without LCF	2.466	1.000	0.746
With LCF	2.484	1.018	0.765
Percentage increase	0.16%	1.81%	2.48%

Table 6.4: Damage to the tower.

As can be seen, the difference in damage due to LCF is almost independent of the detail category used.

6.3.2 Composite material: Blades

From Equation 3.1 it can be seen that the Wöhler coefficient, m, is of great influence, since it is powering the the stress range. For most construction steel, the m coefficient ranges in the order of 3-5, but for other materials it can differ significantly. Composite materials, which are used for most wind turbine blades, can reach m-values up to 6-10. Different values of m and K are therefore found from [Sørensen, J. D. and Toft, H. S. , 2010], for which the damage is found to see what impact LCF makes for composite materials. The damage is found using a representative linear SN-curve, since composite material only operate with this. The results can be seen in Table 6.5. The design parameter is fitted for each case of m and K values, without Low cycle Fatigue. The required z-parameter for a design including Low cycle Fatigue, resulting in a damage of 1 can be seen in Table 6.5 as well.

	m=6.719 K=21.359	m=10.541 K=27.768
SN-curve	Linear	Linear
Damage, without LCF	1	1
Damage, with LCF	1.07	1.26
Percentage increase	7%	26%
z-parameter, without LCF	450	698
z-parameter, with LCF	454	713
Percentage increase	0.9%	2.1

Table 6.5: Damage for composite material

As expected, the impact on the damage is seen to accelerate rather quickly when increasing the Wöhler coefficient. The underestimation of the fatigue damage by up to 26% is of a magnitude that indicates that this issue should be taken into account, when designing composite materials for fatigue.

6.4 Low cycle Fatigue Alternative

The method proposed in [Larsen, G. C. and Thomsen, K , 1996] to include Low cycle Fatigue includes the cycles from the maximum and minimum of 2 consecutive 10 minutes time series, if the mean wind between these series change. However, a large cycle could also occur between the maximum and minimum of 2 consecutive time series, with the same mean wind speed. Another approach to quantify the Low cycle Fatigue load is therefore presented, which take this into account.

An ideal approach would be to perform a rainflow count over a single time series of the length of the life time. The assembling of this time series proves some difficulties, though. The data required to assemble a 20 year response series is, with the sample frequency of 20 Hz, is 365x24x60x60x20x20 = 1.2x10^{1}0. This exceeds the maximum vector size of the program used, [MATLAB, The MathWorks, 2009]. Instead of using 20 a single 20 year series, smaller series of e.g. a year each can be assembled, to counter this problem. This solution falls short to describe the actual load as well, but a significantly improvement is nonetheless achieved. As an alternative, another program with larger data capacity can be used.

Another problem is the linking of the 10 min. series. A "‘jump"’ in wind load is occurring each time a new series is added. This is illustrated at Figure 6.4

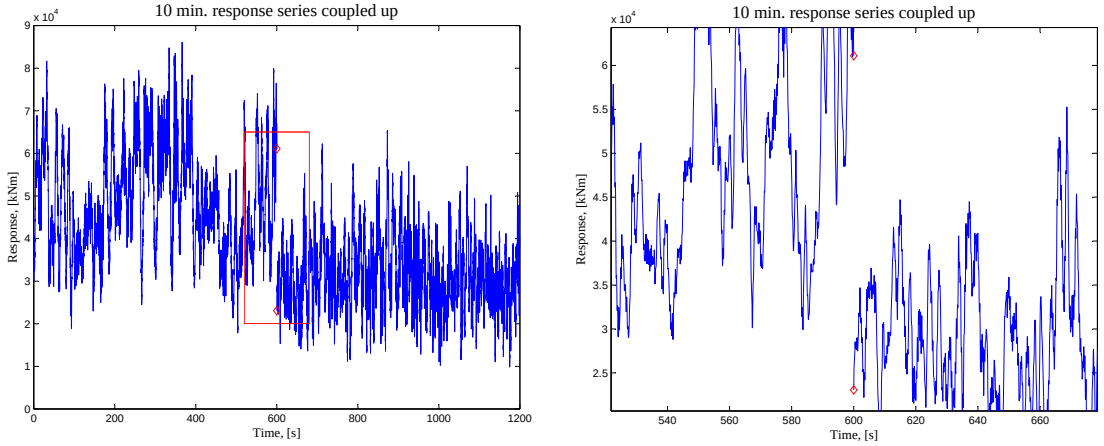

(a) Coupling of two 10 min. series.

(b) Sorted Coupling of two 10 min. series.

Figure 6.4: Coupling of two 10 min. series.

As can be seen, this jump will lead to an unintended stress cycle for each 10 minutes interval. To avoid the issues with the heavy data handling and the jump in stresses when coupling the time series, another approach is proposed. Inspired by the algorithm presented in [Larsen, G. C. and Thomsen, K , 1996], the minimum and maximum for each of the 10 min. series are identified, and assembled in a separate load series. By using the order of mean wind speeds from Horns Rev, described in Section 6.3, a new series is assembled for which a rainflow counting can be done to find the stress cycles. This way, the largest cycles from the entire lifespan of the wind turbine is included. Some cycles will however be included, that already are counted. These cycles are the ones running from maximum to minimum in each 10 min. series. This means that this method will result in a too large contribution to the fatigue.

The main difference between this method and the one presented in [Larsen, G. C. and Thomsen, K , 1996] is that every minimum and maximum response for the 10 minutes series are extracted regardless of whether a change in mean wind speed is occurring. For convenience, the maximum and minimum values are listed in the order of

max-min-max-mix, regardless of if this is actually the case. This simplification will lead to a larger number of cycles, see Figure 6.5.

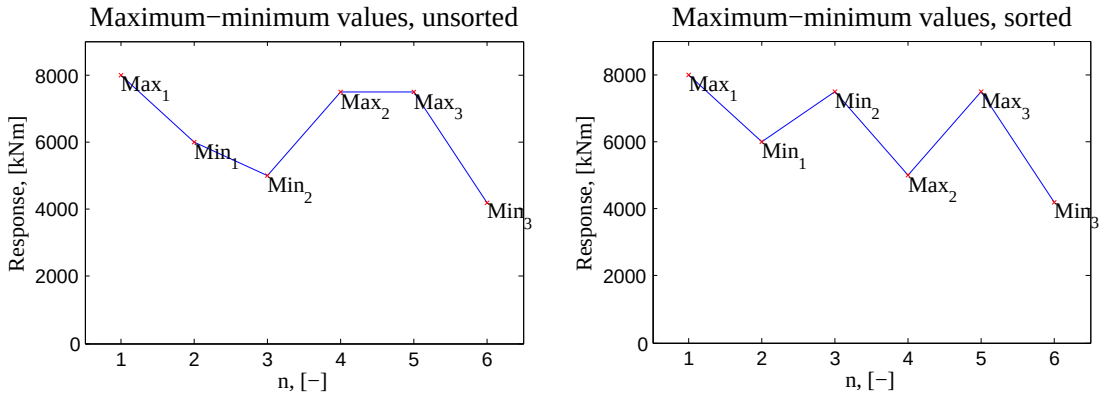

(a) Coupling of three 10 min. series.

(b) Coupling of three 10 min. series, sorted.

Figure 6.5: Coupling of three 10 min. series.

By implementing this theory, the damage can be found by the design equations described in Section 5.2 and 6.2, with a design parameter, z, kept constant. This is done for the case of a linear SN-curve, a bilinear, and a bilinear with cut-off. The results can be seen in Table 6.6.

Parameter	Linear	Bi-linear	Cut-off
Without LCF	2.58	1	0.84
With LCF	2.75	1.18	1.02
Percentage increase	6.6%	18%	21.4%

Table 6.6: Damage to the tower.

If compared with the results in Section 6.3, a significantly increase in damage can be seen.

6.5 Reliability Analysis

Based on the design equations described in Section 6.2, limit state equations can be formulated. These can be seen as Equation (6.2), (6.3) and (6.4), for linear, bilinear, and bilinear w. cut-off respectively.

$$g(t) = \Delta - \sum_{i=1}^{n_U} \sum_{j=1}^{n_Q} tn_{ij} \sum_{s_j \geq \Delta s_D} \frac{s_j^{m_1}}{K_1^C} - \sum_{j=1}^{n_Q} tn_{0j} \sum_{s_j \geq \Delta s_D} \frac{s_j^{m_1}}{K_1^C} = 0 \tag{6.2}$$

$$g(t) = \Delta - \sum_{i=1}^{n_U} \sum_{j=1}^{n_Q} tn_{ij} \left(\sum_{s_j \geq \Delta s_D} \frac{s_j^{m_1}}{K_1^C} + \sum_{s_D \geq \Delta s_j} \frac{s_j^{m_2}}{K_2^C} \right) - \sum_{j=1}^{n_Q} tn_{0j} \left(\sum_{s_j \geq \Delta s_D} \frac{s_j^{m_1}}{K_1^C} + \sum_{s_D \geq \Delta s_j} \frac{s_j^{m_2}}{K_2^C} \right) = 0 \tag{6.3}$$

$$g(t) = \Delta - \sum_{i=1}^{n_U} \sum_{j=1}^{n_Q} tn_{ij} \left(\sum_{s_j \geq \Delta s_D} \frac{s_j^{m_1}}{K_1^C} + \sum_{s_D \geq \Delta s_j \geq s_L} \frac{s_j^{m_2}}{K_2^C} \right) - \sum_{j=1}^{n_Q} tn_{0j} \left(\sum_{s_j \geq \Delta s_D} \frac{s_j^{m_1}}{K_1^C} + \sum_{s_D \geq \Delta s_j \geq s_L} \frac{s_j^{m_2}}{K_2^C} \right) = 0 \tag{6.4}$$

where the stress is found by Equation (6.5)

$$s_j = X_w X_{SCF} \frac{Q_j}{z_j} \tag{6.5}$$

These equations will be used to determine the reliability of the wind turbine due to the extra load contribution found in Section 6.3 and 6.4.

6.5.1 Reliability Analysis RISØ Model

Implementing the LCF from [Larsen, G. C. and Thomsen, K , 1996] in the limit state equations, an updated reliability is found. The stochastic variables used in the equations are defined in Table 6.7. The design parameter, z, is found by the linear design equation, (5.3) for detail category 36.

Parameter	Distribution	Mean value, μ_i	Standard deviation, σ_i
Miners rule, X_Δ	LogNormal	1	0.3
Wind load, X_w	Lognormal	1	0.2
Stress calculation, X_{SCF}	Lognormal	1	0.1
Material parameter, linear part, K_{lin}	Normal	11.3699 + 2x σ_i	0.2
Material parameter, bilinear part, K_{bilin}	Normal	14.2172 + 2x σ_i	0.2

Table 6.7: Stochastic parameters.

A Monte Carlo simulation with 10^5 realisations of the stochastic variables is run, and the accumulated reliability index is found for the 20 year lifetime. The results are plotted at Figure 6.6, as well as the reliability for the wind turbine without LCF. The limit value of the accumulated reliability index, as defined in Table 5.2, are marked as well, both for a linear and bilinear based limit state.

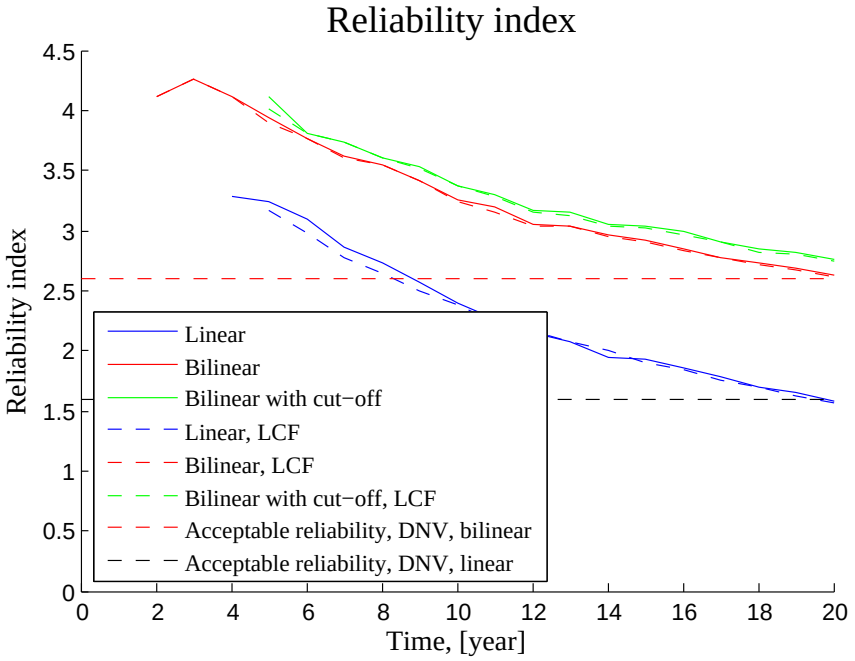

Figure 6.6: Accumulated reliability index for linear, bilinear and bilinear w. cut-off. With and without LCF, RISØ.

From Figure 6.6 it can be seen that the impact of LCF on the reliability of the wind turbine, implemented by the theory described in [Larsen, G. C. and Thomsen, K , 1996], is marginal. As with the reliability analysis in Section

5.2, the Monte Carlo simulation does not provide reliable results the first couple of years. The resulting reliability index can be seen in Table 6.8

Parameter	Reliability index, EC	Reliability index, LCF
Linear	1.58	1.57
Bilinear	2.63	2.62
Bilinear w. cut-off	2.76	2.75

Table 6.8: Z-values for linear and bilinear SN-curves, with and without Low cycle Fatigue, for t = T_L.

As can be seen from Table 6.8, the impact on the reliability index caused by LCF is marginal.

6.5.2 Reliability Analysis, Alternative

Implementing the proposed LCF load found from Section 6.4 in the limit state equations, an updated reliability is found. The stochastic variables used in the limit state equations are defined in Table 6.7. As for the LCF load found by [Larsen, G. C. and Thomsen, K , 1996], a Monte Carlo simulation is run with 10^5 realisations of the stochastic variables, and the accumulated reliability index is found for the 20 year lifetime. The results are plotted at Figure 6.7, as well as the reliability for the wind turbine without LCF. The desired accumulated reliability index according to DNV is marking the desired value.

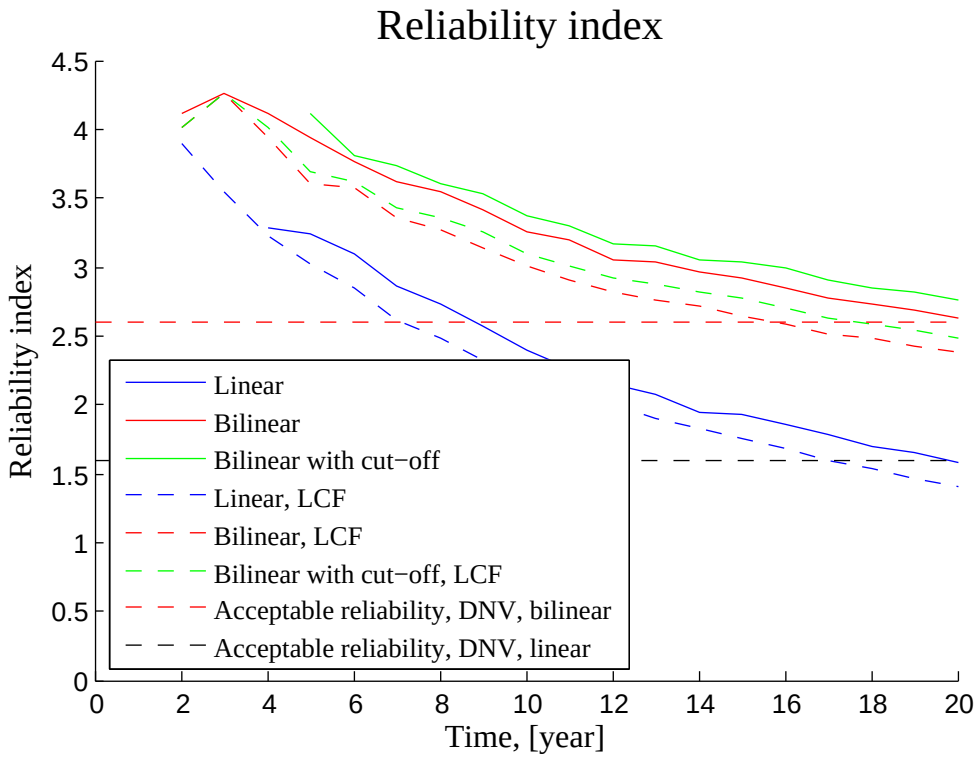

Figure 6.7: Accumulated reliability index for linear, bilinear and bilinear w. cut-off. With and without LCF, Alternative.

From Figure 6.7 it can be seen that the reliability is decreased significant by LCF, implemented by the theory described in Section 6.4. If looking at the reliability based on the bilinear SN-curve, it can be observed that the

code based limit is reached more than 4 years earlier, than if no LCF is included. The damage contribution due to LCF was determined in Table 6.2, and found to increase with the use of a bilinear SN-curve. Hence, tthe reliability index is expected to decrease when a bilinear SN-curve is used, compared to a linear. This proves to be the case indeed, according to Figure 6.7.

6.6 Calabration of FDF

A small study is made to calibrate the partial safety factors, in this case implemented in the Fatigue Design Factor. The z-parameter is determined using different values of FDF, and the resulting accumulated reliability index is found. Results can be seen at Figure 6.8

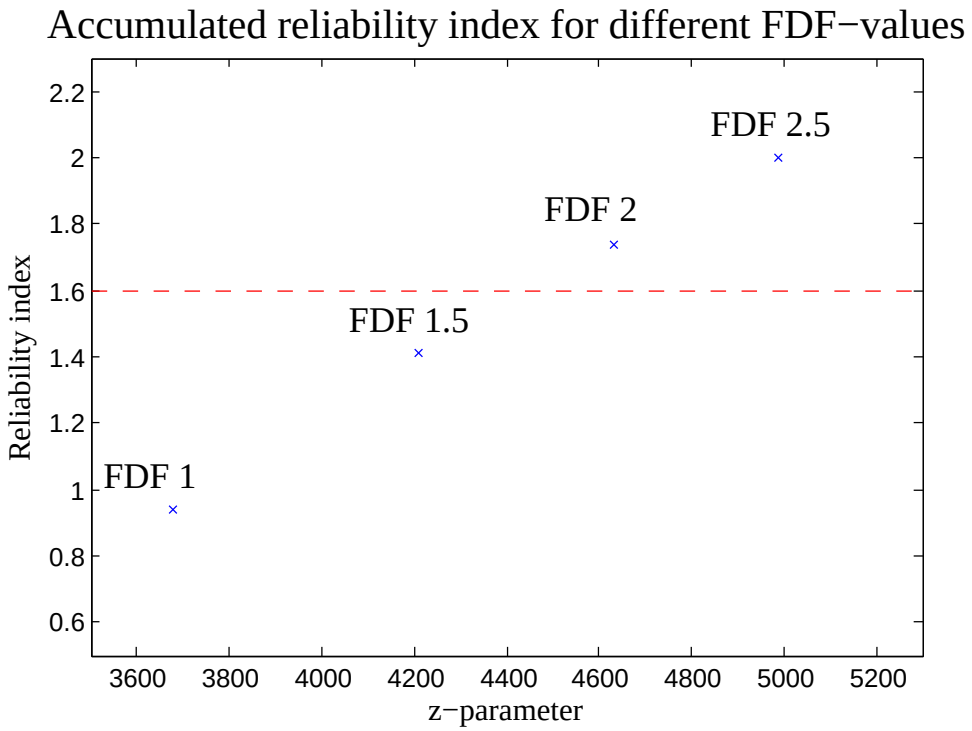

Figure 6.8: Accumulated reliability index for different values of safety factor.

From Figure 6.8, it can be seen that the required reliability is reached by implementing a FDF between 1.5 and 2.0, instead of the 1.5 proposed by the code. This corresponds to a combined partial safety factor, $\gamma_f\gamma_m$ of between 1.15 to 1.25.

6.7 Comments on Low Cycle Fatigue

In the previous sections, two methods have been proposed to include a Low Cycle Fatigue load. The resulting load series of the two methods are of a significantly different magnitude.
The method presented in [Larsen, G. C. and Thomsen, K , 1996] is presenting a load contribution that includes the largest cycle between two consecutive 10 minutes simulated load series. But only if the mean wind of the simulation change, from one 10 minutes series to the next. The drawback of this method is that the cycle ranging from

maximum to minimum in the 10 minutes series is counted twice. Once from the original rainflow counting over the load series, and one more time from LCF. This method identifies some of the stress ranges from low cycles, but might fall short to include the largest ones. The load contribution proposed by this method is therefore expected to be lower than the actual load.
The method proposed in Section 6.4 identifies the largest stress cycles by including the maximum and minimum of each 10 minutes load series, whether a change in mean wind is happening or not. As for the Risø approach, the issue with counting some cycles twice is present. For this method, the error will be larger though, since more maximum and minimums are included. This method is therefore expected to produce a too large load contribution from Low Cycle Fatigue.

The real contribution from LCF is somewhere in between the two methods, so a proper solution on the quantification of the impact of this is not achieved. It is however showed that LCF is an interesting issue, which should be given further attention, due to the large impact obtained in Section 6.4. This is especially the case when dealing with composite materials, since the increase in Wöhler coefficient greatly increase the sensitivity to large stress cycles.

7 Nonlinear SN-curve

In this chapter a non-linear SN-curve is presented and compared with a code based linear. A reliability analysis is performed to analyse the impact of designing with the non-linear curve.

7.1 Introduction

Both Eurocode 3 and DNV-RP-C203 design codes uses the three cases of SN-curves: linear, bilinear, and bilinear with cut-off. The location of the knee point of the SN-curves is important, since even a small change in the location of these can lead to a significant change in damage. This is especially the case if large concentrations of stress ranges are present around this part of the curve. To avoid the abrupt change in the SN-curve, an alternative is presented in [Lassen, T. et al , 2005]. Instead of assuming a linear correlation between the number of cycles and the stress ranges, in a logarithmic scale, a nonlinear curve is fitted. The theory behind the non-linear SN-curve will be briefly explained, and a stochastic modelling of the uncertainties involved will be made, resulting in an analysis of the reliability obtained by designing with this theory.

7.2 Random Limit Fatigue Model

The SN-curve described in [Lassen, T. et al , 2005] is denoted Random Limit Fatigue Model and will further on be referred to as RLFM. The method is proposed due to the large uncertainties on the location of the knee point. To take this into consideration, a nonlinear correlation between stress ranges and number of cycles is proposed, and the uncertainty regarding the location of the knee point is incorporated. This nonlinear correlation is assumed valid for the entire span of stress ranges, instead of only partly, as for the bilinear case. Equation (7.1) describes the nonlinear SN-curve

$$\ln N = \beta_0 - \beta_1 \ln(\Delta\sigma - \gamma) + \varepsilon \tag{7.1}$$

where

N_{0j}	Number of cycles to failure, [-]
β_0	Fitting parameter, [-]
β_1	Fitting parameter, [-]
$\Delta\sigma$	Stress ranges, [MPa]
γ	Fatigue limit, [MPa]
ε	Error term, [-]

The stress ranges, $\Delta\sigma$, are determined by Equation (5.6). The RLFM-curve is fitted to the median of a linear SN-curve from [Det Norske Veritas, 2010], class F, with cut-off. The values used for both can be seen in Table 7.1, and

the resulting SN-curves are shown at Figure 7.1.
To investigate the impact in the reliability, the design parameter, z, is found for a linear SN-curve with cut off. This parameter is then used in the limit state equation for the RLFM case.

Parameter	Value
β_0	22.480 [MPa]
β_1	2.1 [-]
γ	4.1 [MPa]
ε	0 [MPa]
m_{linear}	3 [-]
$\log K_{linear}$, median	12.255[-]
$\log K_{linear}$, 97.7 fractile	11.855[-]
n_L	$5x10^6$
FDF	2

Table 7.1: Data for SN-curves, RLFM and bilinear

The error term, ε, is used later, when modelling the SN-curve with stochastic variables. The $\log K$-value describing the median curve is found by Equation (7.2)

$$\log K_{characteristic} = \log K_{median} + 2\sigma_{\log K} \tag{7.2}$$

where

σ	Standard deviation, $\log K$

The standard deviation is assumed to be 0.2.

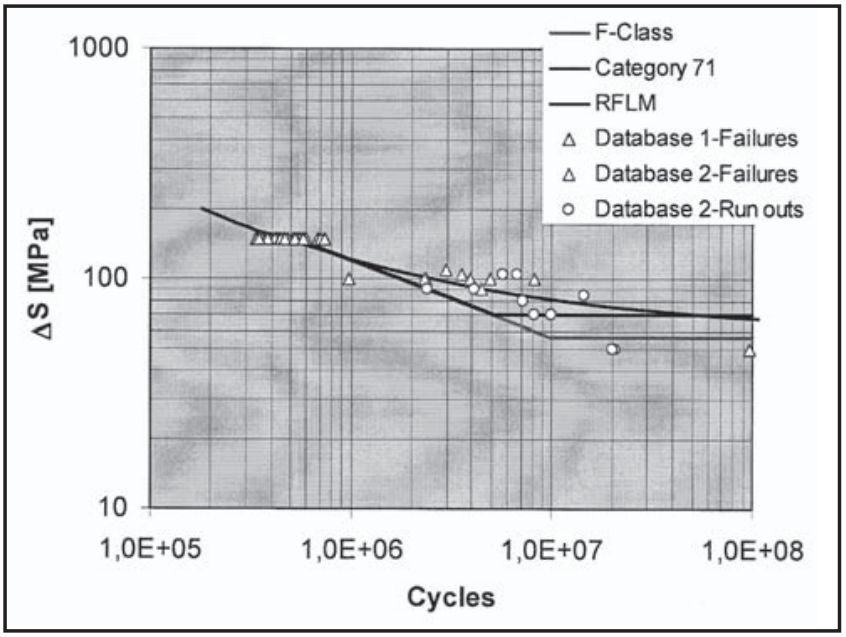

Figure 7.1: RFLM and fitted median curve from DNV and Eurocode 3 [Lassen, T. et al , 2005].

The database values at Figure 7.1 are test data from which the linear SN-curve for F-class details in [Det Norske Veritas, 2010] are formed. As can be seen from Figure 7.1, the RLFM curve fits rather well with the test data. It

can also be seen that the bilniear SN-curve is much more conservative, especially around the knee point, whereas for high and low stress ranges, they more or less agree.

7.2.1 Design Equation DNV F-class SN-curve

Since the RLFM is fitted to the F-class from [Det Norske Veritas, 2010], linear SN-curve with cut-off, this SN-curve is used in the design equation. This equation can be seen at Equation (7.3). The used FDF and K-value, 97.7% fractile of logK, can be seen in Table 7.1.

$$G = 1 - \sum_{i=1}^{n_U} \sum_{j=1}^{n_Q} T_L n_{ij} FDF \sum_{s_j \geq \Delta s_L} \frac{s_j^{m_1}}{K_{linear}} = 0 \tag{7.3}$$

where

s_L	Stress, cut-off, [MPa]
FDF	Fatigue Design Factor, DNV

The Fatigue Design Factor according to [Det Norske Veritas, 2007] set to 1.5 and 2.0 for a linear and bilinear SN-curve respectively. These values are based on the assumption that failure of the detail is critical, and that inspections are possible. The resulting z-value can be seen in Table 7.1, with a FDF of 1.5.

7.2.2 Design Equation, RLFM

A design equation is assembled based on RLFM as well. No data was available for the authors of this thesis, so the 97.75% fractile RLFM based SN-curve is only fitted visiualy. The fitted curve is shown at Figure 7.2, and the parameters describing it can be seen in Table 7.2

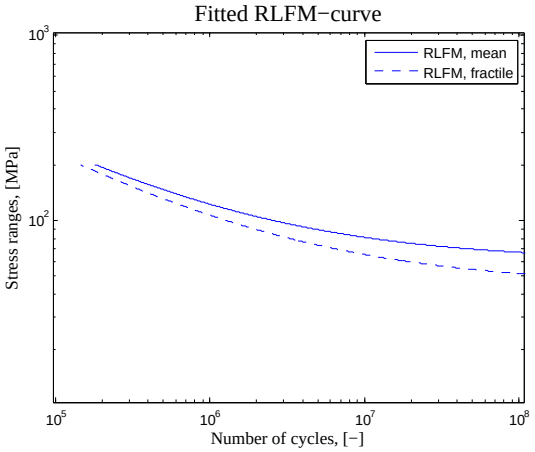

(a) Mean and fitted fractile SN-curve, based on RLFM

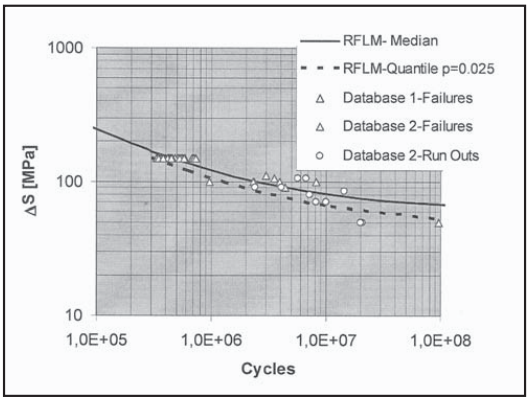

(b) Mean and fractile SN-curve by [Lassen, T. et al , 2005]

Figure 7.2: RLFM based SN-curves.

To fit the fractile curve, the only parameter changed is the limit stress, γ, as can be seen in Table 7.2

Parameter	Value
β_0	22.480 [MPa]
β_1	2.1 [-]
$\ln\gamma$	3.8 [MPa]
ε	0 [MPa]

Table 7.2: Data for fractile RLFM based SN-curve

The design equation can now be assembled, from which the z-parameter can be determined. This is done in Equation (7.4)

$$g = 1 - \sum_{i=1}^{nU} \sum_{j=1}^{nQ} \frac{FDF\, n_{ij} T_L}{exp(\beta_0 - \beta_1 log(s_j - \gamma)) + \varepsilon} \tag{7.4}$$

The FDF is not previously defined for a RLFM based SN-curve, so initially, this is set to 1. A further analysis will be made for calibration of this, to ensure an acceptable safety when using this design equation.

7.2.3 Comparison of Design Equations

The SN-curves used for the design equations can be seen at Figure 7.3, as well as the mean curves. It can be seen that for stress ranges between 70 and 130 MPa the RLFM predict less damage than the linear with cut-off.

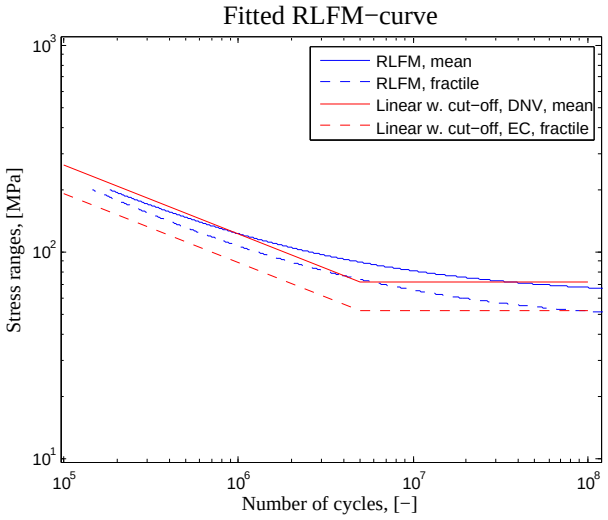

Figure 7.3: Mean and fractile SN-curves, linear w. cut-off and RLFM

To compare the design equations, z-values are found for both. The FDF used is set to 1.0 in this case, and the results can be seen in Table 7.3

Parameter	Value
z_{RLFM}	913 [m^3]
z_{lin}	1487 [m^3]

Table 7.3: Data for SN-curves, RLFM and bilinear

The design by linear SN-curve is seen to give a z-parameter much larger than by RLFM. These values are used later in the reliability analysis. Figure 7.3 shows the large reliability implemented in the code, compared to the RLFM proposed. The difference between the characteristic and mean curves can be seen to larger than for the RLFM, especially for the higher stress ranges. For the linear w. cut-off based design curve it is worth noticing the location of the cut-off. This is expected to have a significant influence on the reliability, since a large part of the stress ranges is below the cut-off value.

7.3 Reliability Analysis

Based on the SN-curve described in Section 7.2, a limit state equation can be formulated. This can be seen as Equation (7.5).

$$g(t) = \Delta - \sum_{i=1}^{nU} \sum_{j=1}^{nQ} \frac{n_{ij} t}{exp(\beta_0 - \beta_1 log(s_j - X_\gamma) + X_\varepsilon} \tag{7.5}$$

where the stress is found by Equation (7.6)

$$s_j = X_w X_{SCF} \frac{Q_j}{z_j} \left(\frac{T}{T_{ref}} \right)^{\alpha} \tag{7.6}$$

This limit state equation will be used to determine the reliability of the wind turbine, when RLFM is implemented. The stochastic variables and design parameters can be seen in Table 7.4. For comparison, a limit state equation based on a linear SN-curve with cut-off from [Det Norske Veritas, 2010] is defined as well. This can be seen at Equation (7.7), and the data used as input can be seen in Table 7.4.

$$g(t) = \Delta - \sum_{i=1}^{n_U} \sum_{j=1}^{n_Q} t n_{ij} FDF \sum_{s_j \geq \Delta s_D} \frac{s_j^{m_1}}{K_1^C} = 0 \tag{7.7}$$

The stresses are found by Equation 7.6.

Parameter	Distribution	Mean value, μ_i	Standard deviation, σ_i
X_Δ	Lognormal	1	0.3
X_w	Lognormal	1	0.2
X_{SCF}	Lognormal	1	0.1
$\ln\gamma$	Normal	4.1	0.16
ε	Normal	0	0.14
$\log K_{lin}$	Normal	11.3699	0.2
z_{linear}	Deterministic	1487	-
z_{RLFM}	Deterministic	913	-

Table 7.4: Stochastic parameters.

The index on the design parameters, z, states which design equation has been used to determine it.

7.3.1 Reliability Analysis, DNV-RLFM

The reliability of the wind turbine is analysed by running a Monte Carlo simulation of the limit state equation based on RLFM, from Equation (7.5). The design parameter is found by the linear SN-curve with cut-off from

[Det Norske Veritas, 2010], see Equation (7.3). 10^5 realisations of the stochastic variables are made, and the resulting reliability can be seen at Figure 7.4

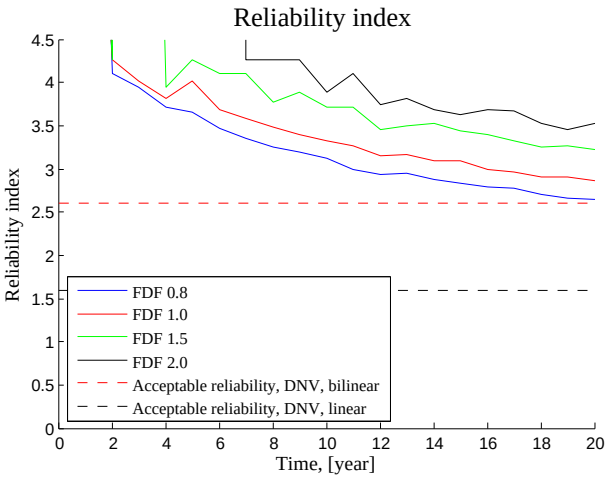

Figure 7.4: Accumulated reliability index, RLFM based

It can be seen that a very low FDF is required to provide the acceptable reliability, according to the one stated in [Det Norske Veritas, 2010]. Implementing a FDF below 1, means effectively that the partial safety factor is reducing the strength of the structure. This indicates that either RLFM is overestimating the strength, or the code is too conservative. If looking at Figure 7.1, it can be seen that the mean linear SN-curve is to the left of the majority of the test made. If a more realistic mean curve was to be proposed, the test should be more evenly distributed on each side.

7.3.2 Reliability Analysis, RLFM-RLFM

The reliability of the wind turbine is analysed by running a Monte Carlo simulation of the limit state equation based on RLFM, see Equation (7.5). The design parameter, z, is found by the RLFM based SN-curve, see Equation (7.4). 100000 realisations of the stochastic variables are run, and the results can be seen at Figure 7.5.

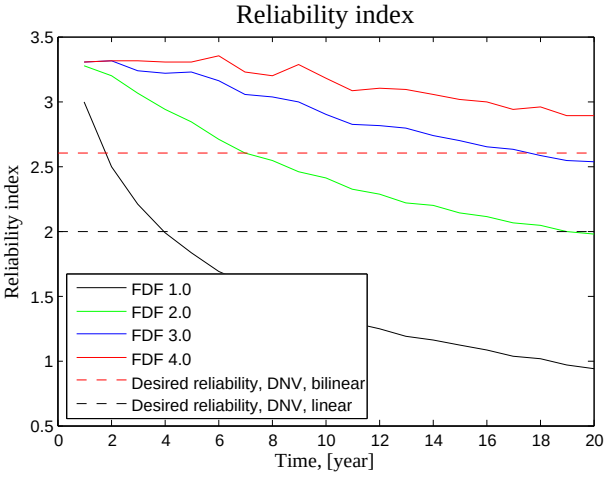

Figure 7.5: Accumulated reliability index, RLFM based

As can be seen, the FDF required to ensure an acceptable reliability index is higher than for a design with the linear

SN-curve.

7.3.3 Reliability Analysis, DNV-DNV

The reliability of the wind turbine is analysed by running a Monte Carlo simulation of the limit state equation based on a linear SN-curve with cut-off, see Equation (7.7). The design parameter, z, is found for the same case of SN-curve, see Equation (7.3). 100000 realisations of the stochastic variables are run, and the results can be seen at Figure 7.6.

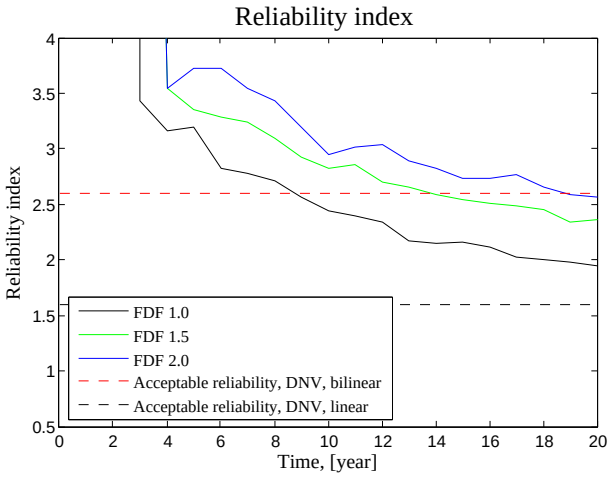

Figure 7.6: Accumulated reliability index, DNV based

From Figure 7.6 it can be seen that the reliability achieved is significantly smaller than by using the limit state equation based on RLFM. This is due to the knee point of the linear SN-curve with cut-off, which accumulates more damage than RLFM in the same stress ranges. See Figure 7.3 for visualisation.

7.4 Comments on Random Limit Fatigue Model

As can be seen from Figure 7.4, the FDF of 2 results in an acceptable reliability, according to the code proposed. This is as expected, since both the design and limit state equation is based on SN-curves from the code. When comparing with the reliability obtained when using the RLFM-based limit state equation, see Figure 7.4, the resulting reliability is however seen to be of a much larger magnitude. This shows the potential for improvements by a better modelling of the knee-point.

To show the importance of the knee point, the accumulated reliability can be seen at Figure 7.7 for different cut-off stresses.

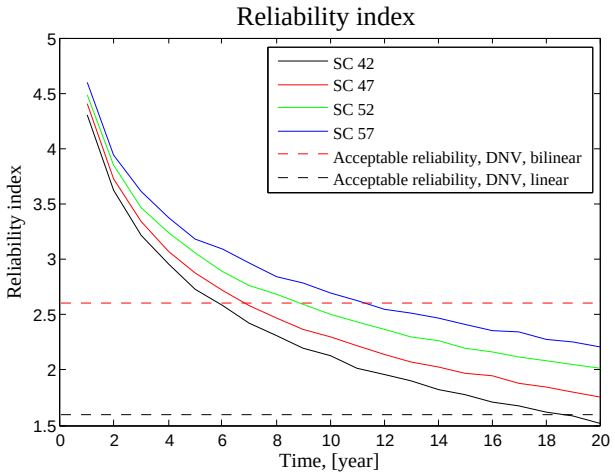

Figure 7.7: Accumulated reliability index.

It can be seen that the reliability is heavily affected by the change in cut-off stress. As illustrated at Figure 7.3, the two design codes does not agree on the location of thee knee point, ranging from a cut-off stress of 52 to 71.

As seen from Figure 7.4, 7.5, and 7.6, a high level of safety is reached when designing for the code based. This is due to the distribution of stress ranges and the location of the knee point. From the comparison of the the design curves at Figure 7.1, it can be seen that for stress ranges below the cut-off, RLFM will predict a higher damage. For comparison, the reliability index is plotted versus the z-parameter for the different SN-curves at Figure

Reliability Analysis of Test Results

8

In this chapter the reliability of the wind turbine tower will be analysed with the results of Test 3, Test 4 and Test 7 to see what influence the different tests have on the reliability.
In order to be able to compare the reliability level for different SN-curves, the design equation will be based on the the characteristic SN-cuve from Eurocode 3 with a detail category 36.

8.1 Limit state equation

Allmost every test in the Background documentation to Eurocode 3 is made in the range of 60 MPa to 250 MPa where the slope of the curve is found to $m = 3$. This is also case for all tests considered in this report and means that the tests only are valid for the linear SN-curve. The design equation is therefore choosen to Equation (5.3). From the design curve in [Eurocode 1993-1-9, 2005] the design parameter, z, is found to 4209.
With a design parameter, z, the limit state equation can be assembled:

$$g(t) = \Delta - \sum_{i=1}^{n_U} \sum_{j=1}^{n_Q} tn_{ij} \sum_{s_j} \frac{s_j^{m_1}}{K_1^C} = 0 \tag{8.1}$$

The stochastic variables in Equation (8.1) are listed in Table 8.1.

Parameter	Distribution	Mean value, μ_i	Standard deviation, σ_i
Miners rule, X_Δ	Lognormal	1	0.3
Wind load, X_w	Lognormal	1	0.2
Stress calculation, X_{SCF}	Lognormal	1	0.1
Material parameter, linear part, K_{lin}	Normal	$\mu_{K_{lin}}$	$\sigma_{K_{lin}}$

Table 8.1: Stochastic parameters.

The mean value and standard deviation describing the material parameter, K_{lin}, are found for each test series individual, and can be seen in Table 3.3.

8.2 Reliability Analysis

In both [Det Norske Veritas, 2010] and [Eurocode 1993-1-9, 2005] the slope of the design curves is set to $m = 3$. In order to compare the test results with the standards it is chosen to investigate the reliability level for Test 3, Test 4 and Test 7 with a fitted slope to $m = 3$.

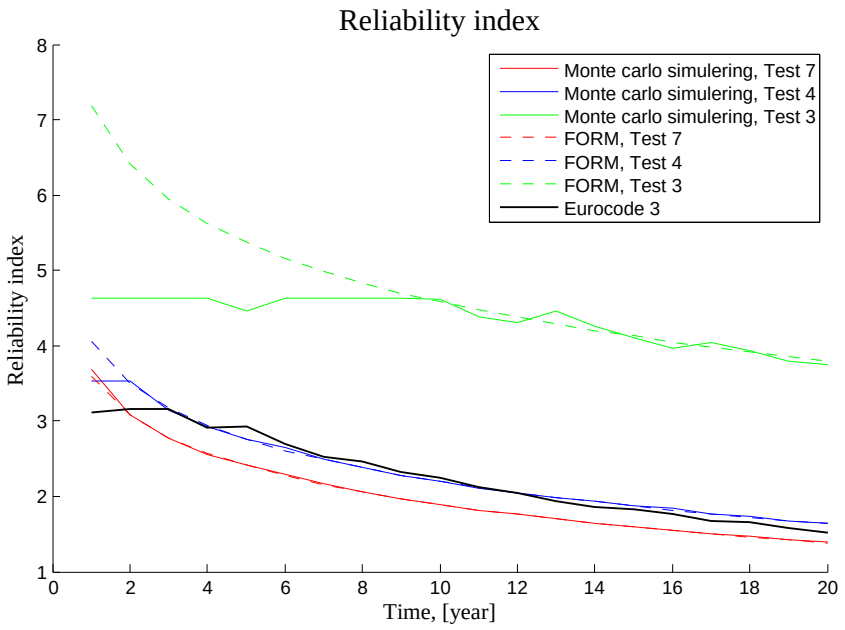

Figure 8.1: Reliability index for Test 3, Test 4 and Test 7

In figure 8.1 the accumulated reliability index is plotted. Here it is seen that the reliability index for Test 3 is very high compared to Eurocode 3. If looked at what was found in Chapter 3 the change in standard deviation when the SN-curve was rotated to $m = 3$ was very small, as well as the scatter around the mean SN-curve. In Chapter 4, this resulted in a high fatigue strength at $2 \cdot 10^6$ cycles, as seen in Table 4.7 for the characteristic SN-curve.
Test 4 and Test 7 have a significantly higher standard deviation when the curve is rotated. Especially Test 7 which is a combination of all other tests and therefore takes different welding methods, steel classes and test specimens into account. This resembles the SN-curve from Eurocode 3 and therefore have a reliability index lying in the same region. In Table 8.2 the accumulated reliability index after 20 years is listed.

Case	β_{acc} by Monte Carlo	β_{acc} by FORM
Test 3	3.75	3.80
Test 4	1.65	1.64
Test 7	1.39	1.38

Table 8.2: Accumulated reliability index.

8.3 Calibration of the Fatigue Design Factor

In Eurocode 3 the Fatigue Design Factor, FDF, is set to 1.5 to include the safety from both loads and fatigue strength. But in Figure 8.1 this is seen to give a very high reliability index for Test 3. It is therefore sought to calibrate the FDF to obtain the required accumulated reliability index, as specified in Table 5.2. In figure 8.2 the FDF is adjusted for Test 3 to see what influence it has on the reliability.

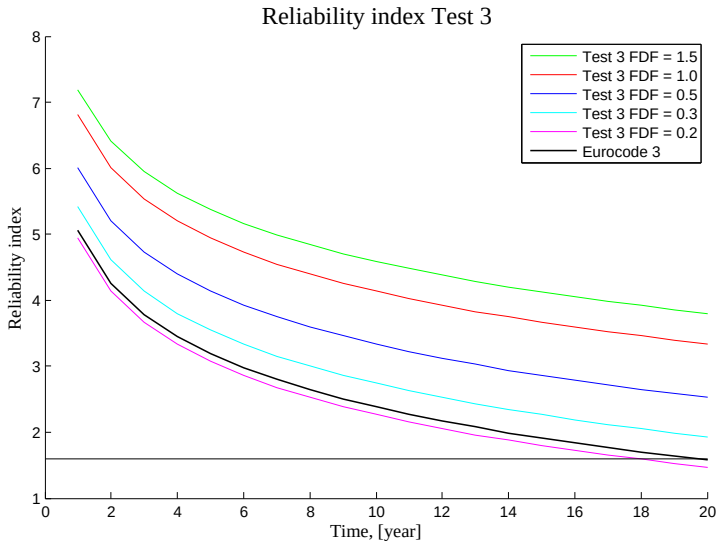

Figure 8.2: Calibration of FDF for Test 3

The target accumulated reliability index β_{acc} is set to 1.6, and it can be seen from figure 8.2 that with a FDF between 0.2 and 0.3 you get an acceptable accumulated reliability index. This shows that a significant reduction in partial safety factors can be made, if test series with low scatter is available. If a FDF of 0.3 is used, this would according to Equation (5.2) effectively lower the product of the partial safety coefficient factors, $\gamma_f\gamma_m$, to 0.67.

To see the effect of a test where the slope is not rotated, the reliability index for Test 1 is calcualted with the specifications listed in table 3.3.
With a slope larger than three it can be seen from Equation (3.1) that the fatigue strength increases, but because of the $\log(K)$ value, which determines where the vertical location is, the strength is not increased compared to Test 3. Interesting is it to see that with the low standard deviation the reliability index is less affected by calibrations of the FDF. The calibration of the FDF for Test 1 can be seen in figure 8.3.

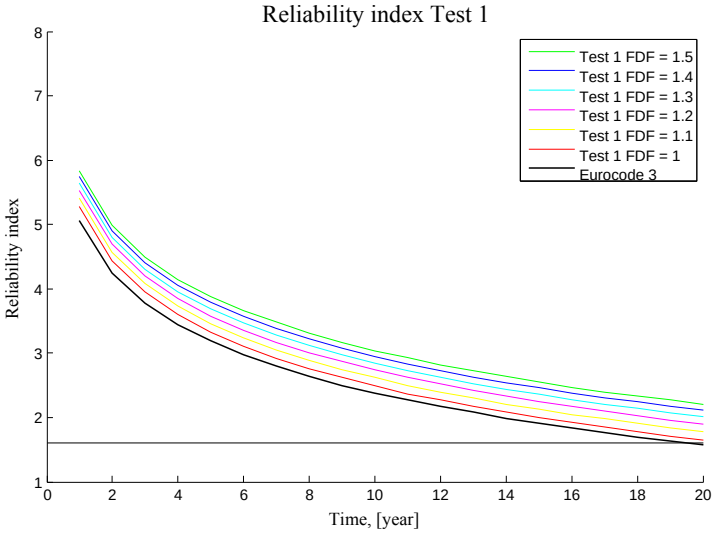

Figure 8.3: Calibration of FDF for Test 1

Still the FDF can be reduced significantly to a value around one. As for Test 3 the test results for Test 1 shows very little scatter around the best fitted curve which gives the small standard deviation, and thereby reduceses the uncertainty of calculating the fatigue strength. This means that if a design is made with a design equation from Eurocode 3, it could be beneficial to make some more accurately fatigue test and thereby obtain a better SN-curve.

9 Sensitivity Analysis

In this chapter a sensitivity analysis is performed for three different design and limit state equations. The influence of the stochastic variables on the reliability index will be investigated to see which uncertainties influence the most.

9.1 Introduction

In the previous chapters the reliability index was derived for different design equations where the uncertainties were modelled by stochastic variables. The impact of how these stochastic variables are modelled is sought analysed, by evaluating the reliability when changing the distribution and/or standard deviation.

9.2 Sensitivity Analysis of δ

To determine the importance of X_δ, three Monte Carlo simulations are made, with the uncertainties defined in Table 9.1, for a linear SN-curve.

Parameter	Distribution	Mean value, μ_i	Standard deviation, σ_i
Miners rule, $X_{\Delta,1}$	Lognormal	1	0.1
Miners rule, $X_{\Delta,2}$	Lognormal	1	0.3
Miners rule, $X_{\Delta,3}$	Lognormal	1	0.5
Wind load, X_w	Lognormal	1	0.2
Stress calculation, X_{SCF}	Lognormal	1	0.1
Material parameter, linear part, K_{lin}	Normal	$10.9699+2\sigma_{K,lin}$	0.2

Table 9.1: Stochastic parameters.

Since X_δ is the stochastic variable subject to the analysis, this is modelled with the three different standard deviations defined in Table 9.1. The accumulated reliability can be seen at Figure 9.1

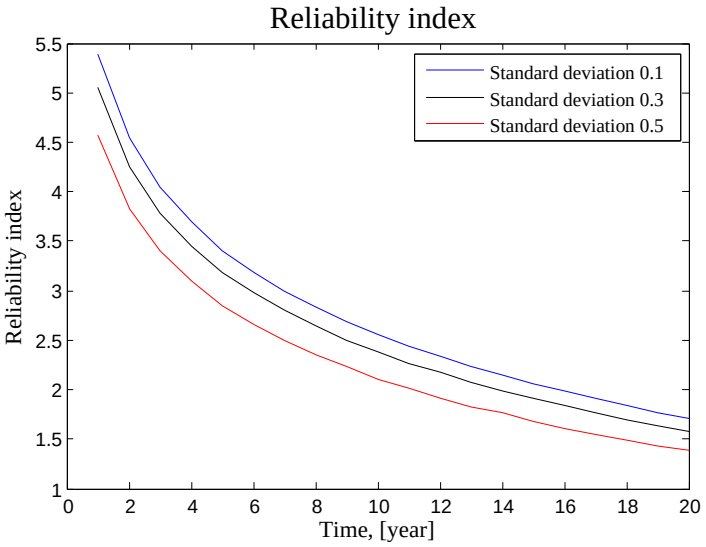

Figure 9.1: Reliability index for different standard deviations of X_δ

From Figure 9.1 it can be seen that the reliability index is decreasing with an increase in standard deviation. This is as expected, since the extreme realisations are causing the failures, and a higher standard deviation affect the magnitudes of these extreme. It is also visualised at Figure 9.2, 9.3, and 9.4, where the concentration of the realisations can be seen to widen up corresponding with an increase in standard deviation.

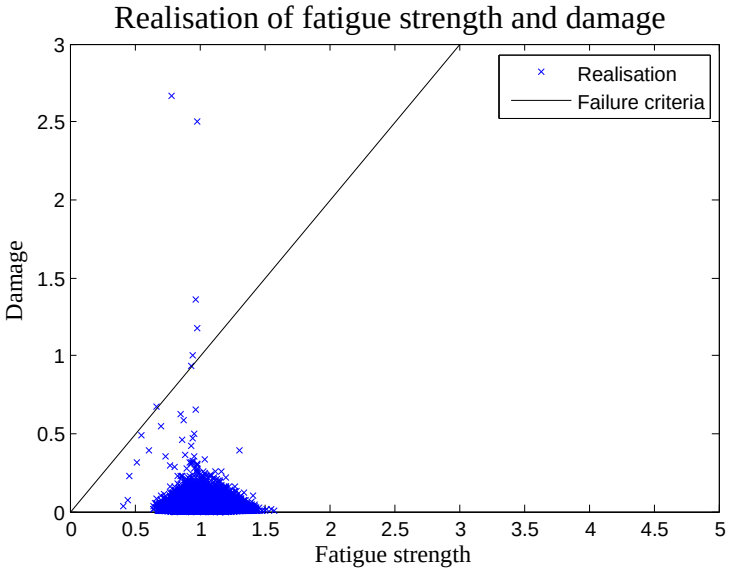

Figure 9.2: Realisations, $\sigma_\delta = 0.1$

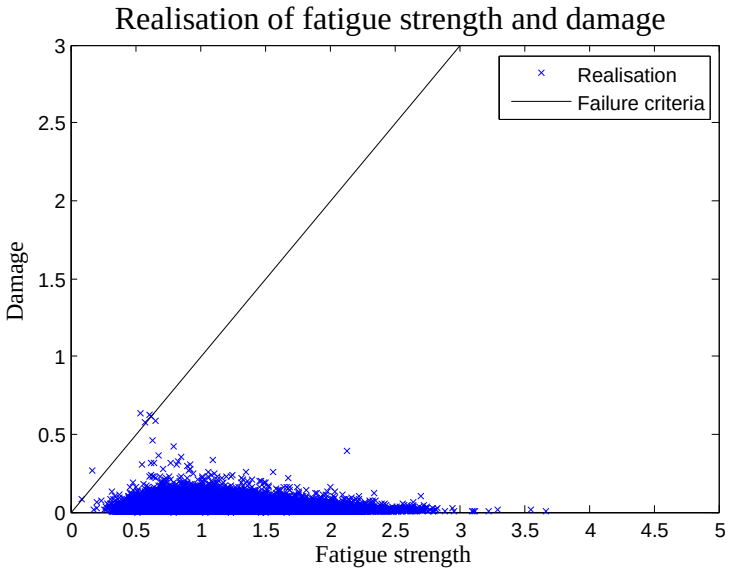

Figure 9.3: Realisations, $\sigma_\delta = 0.3$

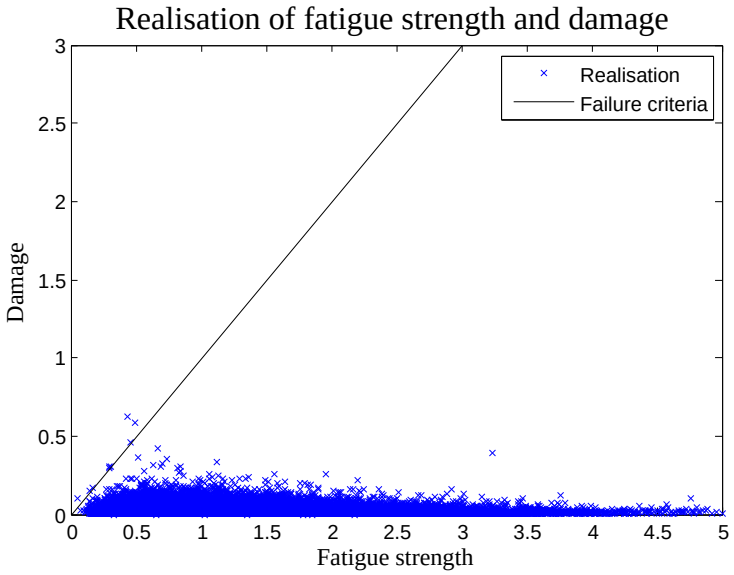

Figure 9.4: Realisations, $\sigma_\delta = 0.5$

It can be seen from the realisations that the influence of σ_δ is significant. This is due to the direct impact on the fatigue strength from the realisation of X_δ, whereas the damage is affected for a number of stochastic variables. This way, a high outcome of a stochastic variable affecting the load can be evened out by outcomes of the other variables.

9.3 Sensitivity analysis of X_{wind}

To determine the importance of X_w, the accumulated reliability index is found with the uncertainties defined in Table 9.2.

Parameter	Distribution	Mean value, μ_i	Standard deviation, σ_i
Miners rule, $X_{\Delta,1}$	Lognormal	1	0.3
Wind load, X_w	Lognormal	1	0.1
Wind load, X_w	Lognormal	1	0.2
Wind load, X_w	Lognormal	1	0.3
Stress calculation, X_{SCF}	Lognormal	1	0.1
Material parameter, linear part, K_{lin}	Normal	$10.9699+2\sigma_{K,lin}$	0.2

Table 9.2: Stochastic parameters.

Since X_w is the stochastic variable subject to the analysis, this is modelled with the three different standard deviations defined in Table 9.2. The accumulated reliability can be seen at Figure 9.5

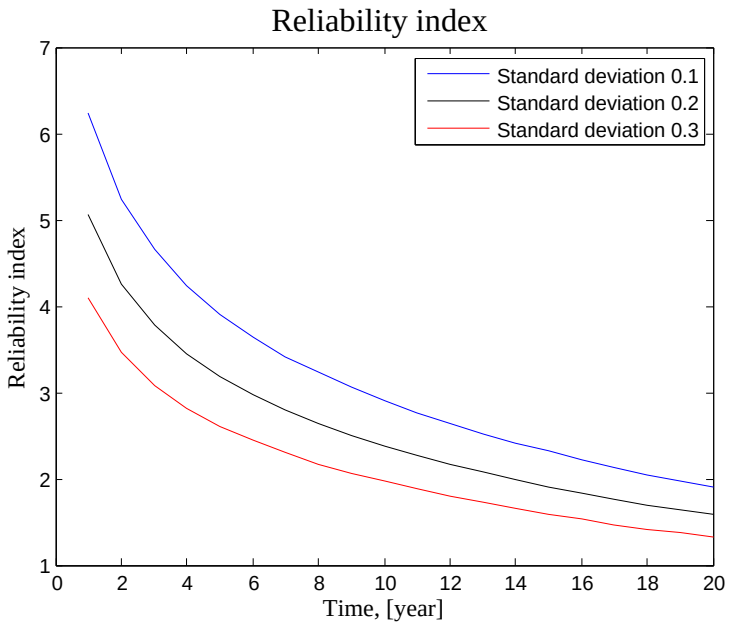

Figure 9.5: Reliability index for different standard deviations of X_w

As for X_δ, an increase of the standard deviation can be seen to decrease the reliability index.

9.4 Sensitivity analysis of K_{lin}

To determine the importance of K_{lin}, the accumulated reliability index is found with the uncertainties defined in Table 9.3.

Parameter	Distribution	Mean value, μ_i	Standard deviation, σ_i
Miners rule, $X_{\Delta,1}$	Lognormal	1	0.3
Wind load, X_w	Lognormal	1	0.2
Stress calculation, X_{SCF}	Lognormal	1	0.1
Stress calculation, X_{SCF}	Lognormal	1	0.1
Material parameter, linear part, K_{lin}	Normal	$10.9699+2\sigma_{K,lin}$	0.1
Material parameter, linear part, K_{lin}	Normal	$10.9699+2\sigma_{K,lin}$	0.2
Material parameter, linear part, K_{lin}	Normal	$10.9699+2\sigma_{K,lin}$	0.3

Table 9.3: Stochastic parameters.

Since K_{lin} is the stochastic variable subject to the analysis, this is modelled with the three different standard deviations defined in Table 9.2. The accumulated reliability can be seen at Figure 9.6

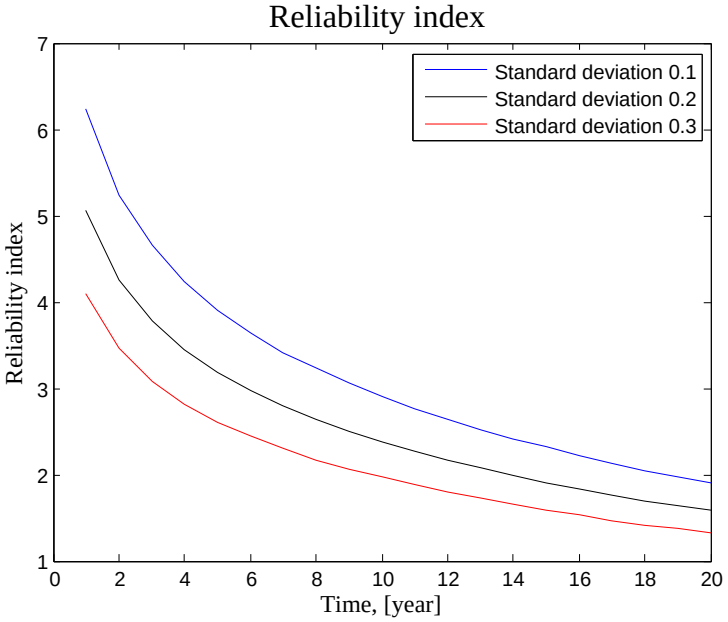

Figure 9.6: Reliability index for different standard deviations of K_{lin}

From Figure 9.6 it can be seen that an increase of the reliability index is caused by an increase in the standard deviation of K_{lin}. This is due to method used to model the mean curve for K_{lin}.

9.5 Comparison

To compare the influence of each of the three analysed stochastic variables, Figure 9.7

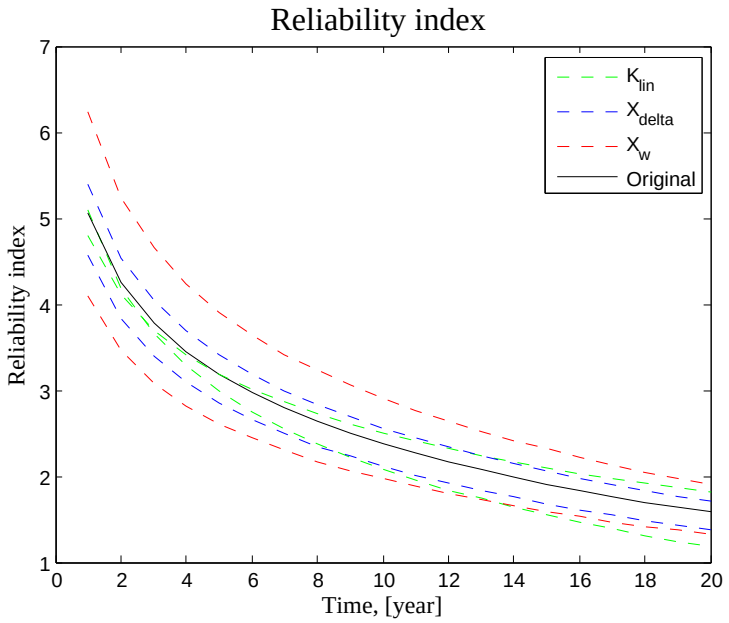

Figure 9.7: Reliability index for different standard deviations of $X\Delta$, X_w and K_{lin}

It can be seen that the largest impact on the reliability is caused by an increase in the standard deviation of K_{lin}.

For a case of bilinear SN-curve and bilinear with cut-off, the trend is found to correspond with the linear case. This can be seen in Appendix 12

Conclusion

10

The aim of this master thesis was to estimate the structural reliability of an off shore wind turbine tower with respect to fatigue loads namely low cycle fatigue. Further more the uncertainties regarding SN-curves and their use was to be analysed with a probabilistic apporach.

With nine years of messurements from Horns reef II a weibull distribution was fitted to the data to get a yearly distribution of the mean windspeeds from 3 m/s to 25 m/s in bins of 2 m/s. By the software TurbSim, six wind fields for each mean wind speed was simulated and randomly picked for the assembly of the wind for one year. The one year of simulated wind fields was then put through another software program, FAST, and the response of a 5 MW wind turbine was calculated. From FAST, the output in the form of a tower bending moment was extracted to analyse the stress ranges in the tower.

In order to calcucalte the fatigue strength, SN-curves is the most common way to describe the relationship between the magnitude of stress ranges, and the number of stress cycles until failure. SN-cuves are found from numerous tests and in [G. Sedlacek et al., 2002], the tests used to determine the design SN-curves in [Eurocode 1993-1-9, 2005] are found. From all tests in this background document, the slopes for a bilinear SN-curve is determined to 3 and 5 for the first and second part. Because the SN-curves in [Eurocode 1993-1-9, 2005] are made from all kinds of different tests and welding methods, these are implemented with a lot of conservatism, to ensure a wide usage. In Chapter 3, the general uncertainties were investigated, for six tests and then for a seventh test, combining all six. It could be confirmed that both slope and location of the curve is influenced by a large natural variation, that is difficult to improve.

Eurocode 3, Det Norske Veritas and The Background Documentation to Eurocode 3 have all three a different method for calculating a characteristic SN-curve from tests. These methods are listed in Table 4.2. In Chapter 4 the methods were used to calculate the characteristic SN-curves for all seven tests. It could be concluded that all methods agrees fairly well with each other by looking at the fatigue strength at $2 \cdot 10^6$ cycles. By rotating the curves to a common slope so that $m = 3$, the curves which had a slope of $m < 3$ got a less conservative strength for cycles of stress ranges less than 100 MPa.

As stated in the introduction, one of the scopes in this thesis was to investigate the significance of Low Cycle Fatigue. The issue occurs when the wind is modelled in series of 10 minutes and then assembled for the entire lifetime. Large cycles gets "lost" when 10 minute series are evaluated individually. An algorithm from [Larsen, G. C. and Thomsen, K , 1996] is therefore implemented, and the reliability index is calculated both with and without the contribution.
Both the literature and our findings shows that the contribution is of little influence. The damage is increased by up to 2.48 % with a bilinear SN-curve with cut-off, and changing the detail category does not make any significant difference. If another material is used with a Wühler coefficient of 10, which is the composite material used in the blades, the results are increased. Here the damage is increased up to 26 % which indicates that LCF needs to be considered.
For the damage in the tower caused by cyclic loading an alternative algorithm is used where every minimum and maximum stress cycle from each 10 minute wind series is used. This algorithm may over estimate the total num-

ber of cycles but still gives an improved contribution of the large cycles, which occur with a low frequency. This method predict an extra load contribution, causing the accumulated reliability index to reach the maximum allowed 4 years before intended, if designed without LCF taken into account. The alternative algorithm to low cycle fatigue may overestimate the damage and the algorithm from [Larsen, G. C. and Thomsen, K , 1996] is deemed to under estimate. In the authors opinion, the real contribution fro LCF lies somewhere in between the two loads proposed.

In chapter 7 a nonlinear SN-curve is proposed by [Lassen, T. et al , 2005]. This is done to avoid the knee point in the bilinear SN-curve from Eurocode 3. The location of the knee point can have a critical impact on the reliability, but by using the Random Limit Fatigue Model this can be decreased. Instead, a stochastic variable, γ, models the fatigue limit. This combined with a nonlinar form of the curve gives a less conservative estimation on the fatigue damage. By designing with the SN-curve proposed by the code and implementing a limit state equation based on RLMF, a FDF can be applied which is below one. This corresponds effectively to implement partial safety factors below one as well. The product of the partial safety factors, $\gamma_m\gamma_f$ is found to 0.92. This illustrates well the safety implemented in the design codes, especially around the knee point.

With the response of the tower found in Chapter 2 the accumulated reliability is calculated for Test 3, Test 4 and Test 7. With the design equation from the linear SN-curve in Eurocode 3, the design parameter z is found. With this design parameter, the accumulated reliability index is calculated with limit state equations for each test. From figure 8.1 is can be seen that the difference between Test 3 and the rest is quite noticeable. The design fatigue factor is calibrated in Figure 8.2 for Test 3, to a value of 0.3 .
From this result, it can be concluded that if a good description of the detail and tests with limited scatter are available, significant reduction in partial safety factors can be achieved. The safety implemented in Eurocode 3 is large due to the mixed test series being used as background data. If test series are made for the same detail, using the same steel class, a significant reduction in scatter is expected to be achieved.

Wind Distribution

11

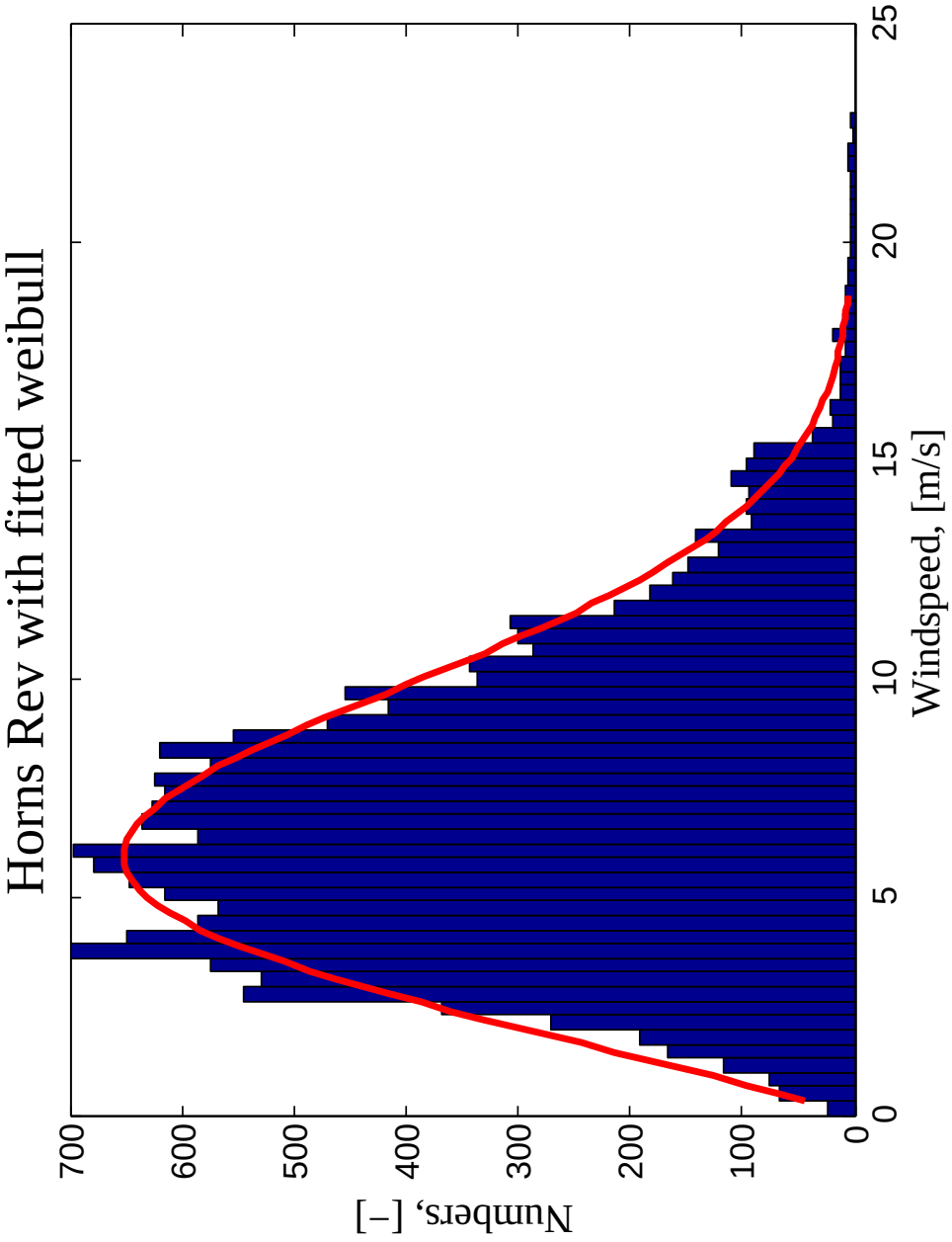

Figure 11.1: Mean wind speed, Horns Rev

Sensitivity analysis 12

12.1 Sensitivity Analysis for a Bilinear SN-curve

In Table

COV_{Δ}	COV_{X_w}	$COV_{X_{SCF}}$	β_{acc}
0.3	0.2	0.1	2.63
0.1	0.2	0.1	2.75
0.2	0.2	0.1	2.70
0.4	0.2	0.1	2.55
0.5	0.2	0.1	2.45
0.3	0.1	0.1	3.52
0.3	0.3	0.1	2.07
0.3	0.4	0.1	1.74
0.3	0.5	0.1	1.53
0.3	0.2	0.2	2.23
0.3	0.2	0.3	1.88
0.3	0.2	0.4	1.64
0.3	0.2	0.5	1.47

Table 12.1: Sensitevity analysis for bi-linear SN-curve.

COV_{Δ}	COV_{X_w}	$COV_{X_{SCF}}$	β_{acc}
0.3	0.2	0.1	2.77
0.1	0.2	0.1	2.89
0.2	0.2	0.1	2.84
0.4	0.2	0.1	2.69
0.5	0.2	0.1	2.60
0.3	0.1	0.1	3.77
0.3	0.3	0.1	2.17
0.3	0.4	0.1	1.81
0.3	0.5	0.1	1.59
0.3	0.2	0.2	2.33
0.3	0.2	0.3	1.96
0.3	0.2	0.4	1.70
0.3	0.2	0.5	1.53

Table 12.2: Sensitevity analysis for bi-linear with cut off SN-curve.

COV_{X_S}	COV_γ	COV_ε	β
0.3	0.16	0.14	1.75
0.3	0.18	0.14	1.71
0.3	0.20	0.14	1.66
0.3	0.40	0.14	1.25
0.3	0.10	0.14	1.86
0.3	0.16	0.16	1.75
0.3	0.16	0.20	1.74
0.3	0.16	0.40	1.71
0.3	0.16	0.50	1.69
0.3	0.16	0.60	1.66

Table 12.3: Sensitevity analysis for Random Limit Fatigue Model.

Bibliography

B. J. Jonkman, M. L. Buhl Jr. FAST. Version: 6.02.

B. J. Jonkman, M. L. Buhl Jr. TurbSim. Version: 1.40.

B. J. Jonkman, M. L. Buhl Jr. (2005). *FAST User's Guide*. National Renewable Energy Laboratory.

B. J. Jonkman, M. L. Buhl Jr. (2008). *TurbSim User's Guide for Version 1.40*. National Renewable Energy Laboratory.

Bilal M. Ayyub et al. (1997). *Probability, Statistics, and Reliability for Engineers and Scientists*. Chapman and Hall.

Det Norske Veritas (2007). *Design of offshore wind turbine structures*.

Det Norske Veritas (2010). *Fatigue Design of Offshore Steel Structures*. Det Norske Veritas.

Dyrbye and Hansen (1997). *Wind Loads on Structures*. Number 2. edition. Wiley.

Eurocode 1993-1-9 (2005). *Design of steel structures - Part 1-9: Fatigue* (2. udgave ed.). CEN.

G. Sedlacek et al. (2002). *1 st. Draft of the Background Document prEN 1993-1-9* (1. ed.). RWTH.

H. S. Toft (2009). *Lecture 8, Lecture notes, Probability Theory and statistics*. Department of Civil Engineering.

Henrik S. Toft (2011). *Lecture notes*. Department of Civil Engineering Aalborg University.

International Electronical Commission (2005). *Wind Turbines - Part 1* (3. edition ed.). IEC.

J. D. Sørensen (2003). *Bestemmelse af karakteristiske værdier for materialeparametre*. Instituttet for Bygningsteknik.

J. D. Sørensen (2004). *Notes in Structural Reliability Theory And Risk Analysis*. Number 2. edition. Aalborg Universitet.

J. D. Sørensen (2011). *Reliability-based calibration of fatigue safety factors for offshore wind turbines*. Department of Civil Engineering Aalborg University, Wind Energy Division Risø-DTU, DK.

J. U. Andersen, R. D. Brandstrup (2003). *Udmattelsesanalyse af bøjningspåvirkede kantsømme i forbindelse med doublerpladesamling*. Aalborg Universitet.

Larsen, G. C. and Thomsen, K (1996). *Low cycle fatigue Loads*. Risø National Laboratory.

Lassen, T. et al (2005). *Fatigue Behavior of Welded Joints Part 1 — Statistical Methods for Fatigue Life Prediction*. American Welding Society and Welding Research Council.

MATLAB, The MathWorks (2009). MATLAB.

Sørensen, J. D. and Toft, H. S. (2010). *Probalistic Design of Wind Turbines*. Risø National Laboratory.

Vestas (2012). *Vestas lifetime*. URL:http://www.vestas.com/da/%C3%A5rsrapport-2011/ledelsesberetning/milj%C3%B8/as-green-as-it-gets/livscyklusvurdering.aspx. Besøgt: 12.04.2012.

List of Corrections